



HAL
open science

Replicating a renewal process at random times

Claude Godrèche, Jean-Marc Luck

► **To cite this version:**

Claude Godrèche, Jean-Marc Luck. Replicating a renewal process at random times. 2023. cea-04265902

HAL Id: cea-04265902

<https://cea.hal.science/cea-04265902>

Preprint submitted on 31 Oct 2023

HAL is a multi-disciplinary open access archive for the deposit and dissemination of scientific research documents, whether they are published or not. The documents may come from teaching and research institutions in France or abroad, or from public or private research centers.

L'archive ouverte pluridisciplinaire **HAL**, est destinée au dépôt et à la diffusion de documents scientifiques de niveau recherche, publiés ou non, émanant des établissements d'enseignement et de recherche français ou étrangers, des laboratoires publics ou privés.

Replicating a renewal process at random times

Claude Godrèche and Jean-Marc Luck

Abstract We replicate a renewal process at random times, which is equivalent to nesting two renewal processes, or considering a renewal process subject to stochastic resetting. We investigate the consequences on the statistical properties of the model of the intricate interplay between the two probability laws governing the distribution of time intervals between renewals, on the one hand, and of time intervals between resettings, on the other hand. In particular, the total number \mathcal{N}_t of renewal events occurring within a specified observation time exhibits a remarkable range of behaviours, depending on the exponents characterising the power-law decays of the two probability distributions. Specifically, \mathcal{N}_t can either grow linearly in time and have relatively negligible fluctuations, or grow subextensively over time while continuing to fluctuate. These behaviours highlight the dominance of the most regular process across all regions of the phase diagram. In the presence of Poissonian resetting, the statistics of \mathcal{N}_t is described by a unique ‘dressed’ renewal process, which is a deformation of the renewal process without resetting. We also discuss the relevance of the present study to first passage under restart and to continuous time random walks subject to stochastic resetting.

1 Introduction

A renewal process is a stochastic model in which events occur randomly over time, resetting the clock for the next event. The interarrival times between events are independent and identically distributed (iid) random variables with a common arbitrary distribution. The Poisson process, which corresponds to choosing an exponential distribution of interarrival times, is the simplest example of a renewal process [1, 2, 3, 4, 5].

In this work, we investigate a theoretical model consisting of two nested renewal processes. The first one—dubbed the internal process—is replicated at random intervals of time, drawn from a distribution characterising the second one—dubbed the external process. The probability density of interarrival times of the internal process will be denoted by $\rho(\tau)$, and that of the external process by $f(T)$. An illustration is provided in figure 1, which depicts five cycles of replication of the internal process, of respective durations T_1, \dots, T_4 and B_t . The last interval, B_t , represents the backward recurrence time, or age of the external process at time t , which is the time elapsed since the last replication event.

To provide a concrete example, in a manufacturing setting, the two nested renewal processes would correspond respectively to the intervals of time between component failures and

Claude Godrèche and Jean-Marc Luck
 Université Paris-Saclay, CNRS, CEA, Institut de Physique Théorique, 91191 Gif-sur-Yvette, France
 E-mail: claude.godreche@ipht.fr, jean-marc.luck@ipht.fr

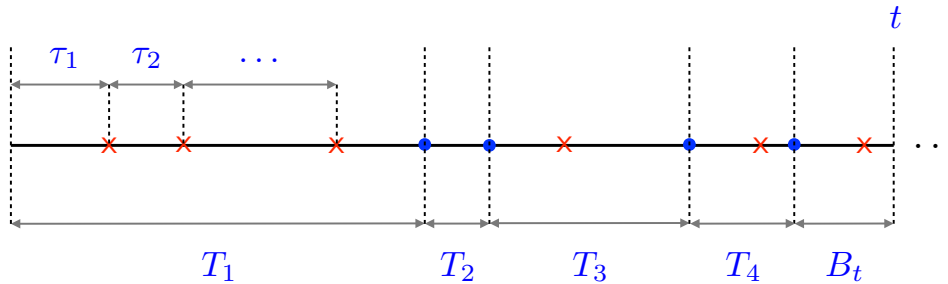


Fig. 1 An example of two nested renewal processes with five cycles of replication of the internal renewal process. Renewal events of the internal process are figured by crosses, replication events (or resettings) due to the external renewal process by dots. The intervals of time between two crosses, τ_1, τ_2, \dots , have common probability density $\rho(\tau)$. The intervals of time between two dots, T_1, T_2, \dots , have common probability density $f(T)$. The last interval, B_t , represents the backward recurrence time or the age of the external process at time t , which indicates the time elapsed since the last replication (or resetting). In this example, the total number \mathcal{N}_t of internal renewals (i.e., of crosses) is equal to 6.

the intervals of time between component replacements. In the context of reliability analysis, the concept of nested renewal processes has been previously introduced in [6], with the following definitions. *Shocks occur to a component randomly in time in an ordinary renewal process, each shock causing a random amount of damage. Damages are identically and independently distributed, and damages resulting from shocks are accumulated. In addition to this cumulative process there is a second ordinary renewal process in time the effect of which is to restart the cumulative renewal process at zero accumulated shocks and consequently zero cumulative damage. This represents component replacement.* This reference will be further examined later. In a broader context, the idea of nesting stochastic processes (not limited to renewal processes) across different scales has been investigated in other disciplines, including the stochastic modeling of precipitation. For example, in [7], an external model is employed to represent the processes related to storm occurrences and the time periods between them, while an internal model nested within it is utilised to capture the variability of rainfall within a given storm.

Interestingly, the model described above, involving two nested renewal processes, happens to be a specific instance of a class of models which has been recently popularised under the name of stochastic processes under resetting. Processes of this type have been studied for a long time, as documented in [8] for a historical perspective. Lately, these models have gained significant attention in the field of statistical physics (see [9, 10] for reviews). One notable aspect of the present study is that the stochastic process subject to resetting is, in fact, a renewal process itself. This (internal) renewal process, characterised by the density $\rho(\tau)$, is reset at random time intervals, which are drawn from the density $f(T)$, characterising the external renewal process.

A simple example of such a process is naturally encountered when considering the simple random walk with steps ± 1 (or Pólya walk [11]) on the one-dimensional lattice, subject to stochastic resetting¹. The events of the internal process are the epochs of the returns to the origin of the walk, while the events of the external process are the reset events in discrete time, corresponding to restarting the walk with a given probability. A companion paper will be entirely dedicated to the study of this process [16]. Another example where such a process is encountered is when considering the continuous time random walk under resetting, as will be commented upon later (see sections 2 and 8).

¹ For reference, other aspects of the Pólya walk, or of more general lattice random walks, subject to stochastic resetting, have been explored in [12, 13, 14, 15].

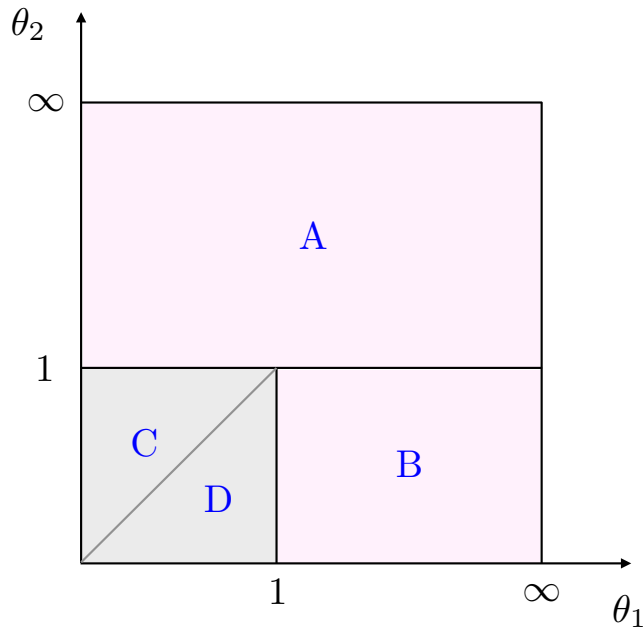


Fig. 2 The four different regions of the phase diagram in the θ_1 - θ_2 -plane. In regions A and B, the number \mathcal{N}_t of internal events (figured by crosses in figure 1) grows linearly with time and has relatively negligible fluctuations around its mean value. In regions C and D, \mathcal{N}_t grows subextensively in time and keeps fluctuating. The notation $\theta_{1,2} = \infty$ refers to thin-tailed distributions that possess finite moments of all orders. Poissonian resetting (see section 6.2) lies on the line $\theta_2 = \infty$.

In this paper, we consider the more abstract model of nested renewal processes in full generality, which implies that we shall allow the two distributions associated with the internal and external renewal processes to be arbitrary². We shall be mostly interested in the case where these distributions have power-law tails with respective exponents θ_1 and θ_2 (see (3.1)).

The main objective of this study is the statistical analysis of the total number of internal events (represented by crosses in figure 1) up to time t , denoted by \mathcal{N}_t . Due to the interplay of two probability distributions, this quantity, despite its apparent simplicity, displays a diverse range of behaviours. These are summarised in figure 2, which illustrates the phase diagram of the model in the θ_1 - θ_2 -plane. In this representation, the symbols $\theta_{1,2} = \infty$ correspond to thin-tailed distributions with finite moments of all orders. This diagram is divided into four distinct regions, exhibiting different asymptotic forms for the statistics of \mathcal{N}_t in the long-time regime of interest.

A remarkable feature of the model emerges from this study. Specifically, we observe that the more regular of the two renewal processes, i.e., the one with the larger of the two exponents θ_1 and θ_2 , always governs the overall regularity of the entire process, as we shall now elaborate.

1. In regions A and B, where the larger exponent is greater than 1, $\langle \mathcal{N}_t \rangle$ grows linearly in time, whereas the fluctuations of \mathcal{N}_t around its mean value are relatively negligible, as in the usual framework of renewal theory in the stationary regime ($\theta > 1$).

More precisely, in region A, such that $\theta_2 > 1$, we have

$$\langle \mathcal{N}_t \rangle \approx \frac{\langle N_{\mathbf{T}} \rangle}{\langle \mathbf{T} \rangle} t,$$

² Reset stochastic processes with arbitrary distributions of the time intervals between resettings have been considered in prior works such as [17, 18, 19, 20, 21, 22, 23].

where $\langle N_{\mathcal{T}} \rangle$ is the mean number of internal events between two resettings, defined in (4.1). In region B, such that $\theta_2 < 1 < \theta_1$,

$$\langle \mathcal{N}_t \rangle \approx \frac{t}{\langle \tau \rangle},$$

with the interpretation that, in this region of the phase diagram, asymptotically, the internal renewal process is not influenced by the external one.

2. In regions C and D, where the larger exponent is less than 1, \mathcal{N}_t grows subextensively in time, with an exponent smaller than unity, and keeps fluctuating, as in the usual framework of renewal theory in the self-similar regime ($\theta < 1$).

More precisely, in region C, where $\theta_1 < \theta_2$, \mathcal{N}_t grows as t^{θ_2} and is asymptotically proportional to the rescaled random variable X_{θ_2} , which is part of usual renewal theory, and whose density $f_{X_{\theta_2}}(x)$ is given by (2.29),

$$\mathcal{N}_t \approx \langle N_{\mathcal{T}} \rangle \frac{X_{\theta_2}}{\Gamma(1 - \theta_2)} \left(\frac{t}{T_0} \right)^{\theta_2}.$$

Thus, \mathcal{N}_t is asymptotically equal to the product of the mean number $\langle N_{\mathcal{T}} \rangle$ of internal events between two resettings by the random number of resettings (see (2.28)).

In region D, where $\theta_1 > \theta_2$, \mathcal{N}_t grows as t^{θ_1} and is asymptotically proportional to a novel rescaled random variable Y_{θ_1, θ_2} ,

$$\mathcal{N}_t \approx \frac{Y_{\theta_1, \theta_2}}{\Gamma(1 - \theta_1)} \left(\frac{t}{\tau_0} \right)^{\theta_1}.$$

The distribution of this dimensionless random variable is universal, depending only on the two exponents θ_1 and θ_2 . Its probability density is depicted in figure 7, for the particular example of $\theta_1 = 1/2$, and for several values of θ_2 .

This dominance of the more regular process also manifests itself in the two special cases where either the internal renewal process, or the external one, are Poisson processes. In both cases, regardless of the distribution of the other process, \mathcal{N}_t exhibits linear growth over time. These two situations are different, though. If the internal process is Poisson, then \mathcal{N}_t is Poisson too, regardless of the distribution of the other process. If the external (resetting) process is Poisson, the statistics of \mathcal{N}_t is exactly described by a single renewal process defined by a dressed density $\rho^{(r)}(\tau)$, whose expression is given in (6.9), in terms of the resetting rate r and of the probability density $\rho(\tau)$ of the internal process. This dressed density is exponentially decaying, regardless of the nature of $\rho(\tau)$. The superscript in $\rho^{(r)}(\tau)$ is an abbreviation for *replication* or *resetting*, terms that we shall use interchangeably.

Beyond the analysis of the statistics of \mathcal{N}_t , a second objective of the present paper is to extend the study to other facets of the model and highlight how the ramifications of the theory connect with other studies. We shall thus be led to consider the question of first-passage time under restart for the process at hand, then revisit some questions related to the study of continuous time random walks under resetting.

The paper is structured as follows. Section 2 provides an overview of key concepts and results in renewal theory that will be used in the subsequent parts of this paper. The material presented there is classical, with the exception of some more specific results. Section 3 gives the precise definition of the process under study, as well as the derivation of the key equation (3.9) for the statistics of \mathcal{N}_t , which is at the basis of subsequent developments. Section 4 contains a detailed description of the phase diagram of the model, summarised above, including all phase boundaries. Section 5 is devoted to the analysis of the asymptotic distribution of \mathcal{N}_t in region D ($0 < \theta_2 < \theta_1 < 1$), and to an in-depth study of the universal distribution of the scaling variable Y_{θ_1, θ_2} . Section 6 applies the previous formalism to two

special cases, where either the internal process, or the external one, are Poissonian. Section 7 deals with the distribution of the first-passage time for the occurrence of a cross (renewal event of the replicated process) in the general case of an arbitrary density $f(T)$, where there is no renewal description of the sequences of crosses. Section 8 is focussed on the number of internal events in the last interval B_t (see figure 1), which is one of the primary quantities analysed in [6], thus extending the scope of the analysis made in this reference to the entire θ_1 - θ_2 -plane. This section also makes the connection of the process under study with continuous time random walks under resetting.

2 Overview of key concepts in renewal theory

This section provides an overview of key concepts and results in renewal theory that will be used in the subsequent parts of this paper. Classical treatments of the subject can be found in [1, 2, 3, 4, 5]. Here we follow the approach presented in [24] and supplement it with some additional material.

2.1 Definition of an ordinary renewal process

Let us consider events occurring at the random epochs of time t_1, t_2, \dots , from some time origin $t = 0$. The origin of time is taken on one of these events. When the intervals of time between events, $\tau_1 = t_1$, $\tau_2 = t_2 - t_1, \dots$, are iid random variables with common density $\rho(\tau)$, the process thus defined is a *renewal process*³. Otherwise stated, τ_2, τ_3, \dots are probabilistic copies of the first time interval τ_1 ⁴. Hereafter we shall use the terms *event* or *renewal* interchangeably.

A simple example of a renewal process in discrete time is given by the times of return to the origin of the Pólya walk mentioned earlier. An even simpler example arises when considering a continuous time random walk (CTRW) [25, 26]. A CTRW is a random walk subordinated to a renewal process. This means that the waiting times between jumps of the walk, are, by definition, the time intervals of a renewal process. The jumps are iid random variables η_1, η_2, \dots , with a distribution independent of that of the waiting times. In the framework of renewal theory a CTRW is a renewal process with reward [3]. The cumulative process considered in [6], recalled above, gives an illustration of a CTRW, where the shocks, causing damages of magnitude η_1, η_2, \dots , correspond to the jumps. The cumulative damage corresponds to the position of the walker. Moreover, as discussed later (see section 8), this process is subject to resettings (replacements in [6]).

The survival probability, that is, the probability that no event occurred up to time t (without counting the event at the origin), is given by

$$R(\tau) = \mathbb{P}(\tau > \tau) = \int_{\tau}^{\infty} dt \rho(t). \quad (2.1)$$

The tail behaviour of this distribution plays a crucial role in the subsequent analysis (and more generally in the study of renewal processes). It induces a distinction between two main classes of distributions, as summarised below.

³ We denote the random intervals of time τ_1, τ_2, \dots by bold letters, and their values in a given realisation of the process by the regular letters τ_1, τ_2, \dots . The same convention applies to the sequence of time intervals T_1, T_2, \dots defined in section 3. This avoids any ambiguity (see, e.g., the comment below (3.3)).

⁴ We do not consider here other cases of renewal processes where the first time interval τ_1 has a different distribution from that of the following time intervals τ_2, τ_3, \dots .

Thin-tailed distributions

If the density $\rho(\tau)$ is either supported by a finite interval, or decaying faster than any power law, all the moments of the random variable τ are finite. The Laplace transform of $\rho(\tau)$, where s is conjugate to τ , is then given by the power series

$$\mathcal{L}_{\tau} \rho(\tau) = \hat{\rho}(s) = \langle e^{-s\tau} \rangle = \sum_{k \geq 0} \frac{(-s)^k}{k!} \langle \tau^k \rangle.$$

More specifically, the above series is convergent if $\rho(\tau)$ either has finite support or decays exponentially or faster, whereas it is only a formal power series if the decay of $\rho(\tau)$ is slower than exponential.

Fat-tailed distributions

If $\rho(\tau)$ is characterised by a power-law fall-off with an arbitrary index $\theta > 0$, parametrising its tail as

$$R(\tau) \approx \left(\frac{\tau_0}{\tau} \right)^{\theta}, \quad (2.2)$$

where τ_0 is a microscopic time scale, we have

$$\rho(\tau) \approx \frac{c}{\tau^{1+\theta}}, \quad c = \theta \tau_0^{\theta}. \quad (2.3)$$

Here, τ has only finitely many moments, as $\langle \tau^k \rangle$ is convergent only for $k < \theta$.

For any value of the index θ that is not an integer, the Laplace transform $\hat{\rho}(s)$ of the density has a singular part as $s \rightarrow 0$, of the form

$$\hat{\rho}(s)_{\text{sg}} \approx c \Gamma(-\theta) s^{\theta}.$$

We thus have

$$\hat{\rho}(s) \approx \begin{cases} 1 - a s^{\theta} & (\theta < 1), \\ 1 - \langle \tau \rangle s + a s^{\theta} & (1 < \theta < 2), \end{cases} \quad (2.4)$$

and so on, with more regular terms as θ lies between higher consecutive integers, and where the positive amplitude a reads

$$a = c |\Gamma(-\theta)| = |\Gamma(1 - \theta)| \tau_0^{\theta}. \quad (2.5)$$

Whenever the index θ is an integer, $\hat{\rho}(s)$ is affected by logarithmic corrections. We mention for further reference the case $\theta = 1$, where we have

$$R(\tau) \approx \frac{\tau_0}{\tau}, \quad \rho(\tau) \approx \frac{\tau_0}{\tau^2}$$

and

$$\hat{\rho}(s) \approx 1 + \tau_0 s \ln(\tau_* s). \quad (2.6)$$

This expression involves, in general, two different microscopic time scales, the amplitude τ_0 (describing the tail of the distribution) and the finite part τ_* (depending on details of the whole distribution).

The class of thin-tailed distributions, where all the moments of τ are finite, corresponds formally to $\theta = \infty$.

2.2 The number N_t of renewals

The number of renewals N_t that occur in the time interval $(0, t)$ satisfies the condition

$$\mathbb{P}(N_t \geq n) = \mathbb{P}(t_n \leq t), \quad (2.7)$$

where the sum of the first n time intervals,

$$t_n = \tau_1 + \tau_2 + \cdots + \tau_n, \quad (2.8)$$

is the waiting time until the occurrence of the n th event, or, for short, the time of the n th renewal. Correspondingly, the time intervals τ_1, τ_2, \dots obey the sum rule

$$\tau_1 + \tau_2 + \cdots + \tau_{N_t} + b_t = t, \quad (2.9)$$

where b_t is the backward recurrence time, or the age of the renewal process at time t , which measures the time elapsed since the last renewal event. The distribution of N_t is given by

$$\begin{aligned} p_n(t) &= \mathbb{P}(N_t = n) \\ &= \int d\tau_1 \dots d\tau_n db \rho(\tau_1) \dots \rho(\tau_n) R(b) \delta\left(\sum_{i=1}^n \tau_i + b - t\right) \\ &= ((\rho \star)^n \star R)(t), \end{aligned} \quad (2.10)$$

where the star denotes a temporal convolution and $(\rho \star)^n$ denotes the n th convolution of the density $\rho(t)$. We have in particular

$$p_0(t) = R(t) \quad (2.11)$$

(see (2.1)). In Laplace space, (2.10) reads

$$\hat{p}_n(s) = \mathcal{L}_t p_n(t) = \hat{\rho}(s)^n \hat{R}(s), \quad (2.12)$$

with

$$\hat{R}(s) = \frac{1 - \hat{\rho}(s)}{s}. \quad (2.13)$$

The distribution of N_t can be expressed compactly through its probability generating function

$$Z(z, t) = \langle z^{N_t} \rangle = \sum_{n \geq 0} z^n p_n(t). \quad (2.14)$$

Using (2.12), (2.13), this yields, in Laplace space,

$$\hat{Z}(z, s) = \mathcal{L}_t \langle z^{N_t} \rangle = \sum_{n \geq 0} z^n \hat{p}_n(s) = \frac{\hat{R}(s)}{1 - z\hat{\rho}(s)},$$

i.e.,

$$\hat{Z}(z, s) = \frac{1 - \hat{\rho}(s)}{s(1 - z\hat{\rho}(s))}. \quad (2.15)$$

Note that $\hat{Z}(1, s) = 1/s$, as it should be. Expressions for the moments $\langle N_t^k \rangle$ in Laplace space can be obtained by differentiating (2.15) with respect to z at $z = 1$. We obtain in particular

$$\mathcal{L}_t \langle N_t \rangle = z \frac{\partial}{\partial z} \hat{Z}(z, s) \Big|_{z=1} = \frac{\hat{\rho}(s)}{s(1 - \hat{\rho}(s))}, \quad (2.16)$$

$$\mathcal{L}_t \langle N_t^2 \rangle = \left(z \frac{\partial}{\partial z} \right)^2 \hat{Z}(z, s) \Big|_{z=1} = \frac{\hat{\rho}(s)(1 + \hat{\rho}(s))}{s(1 - \hat{\rho}(s))^2}. \quad (2.17)$$

2.3 Mean of the single-interval distribution

Another quantity of interest for the sequel is the mean of the single-interval distribution, that is, the distribution of any of the intervals $\tau_1, \tau_2, \dots, \tau_{N_t}$ subject to the condition (2.9). This observable, denoted by τ_t is defined provided that $N_t \geq 1$. In the event where $N_t = 0$, which occurs with probability $p_0(t)$ given by (2.11), τ_t is conventionally set to zero and therefore does not contribute to its mean. We thus have, taking τ_t to be the first interval,

$$\langle \tau_t \rangle = \sum_{n \geq 0} \int d\tau_1 \dots d\tau_n db \tau_1 \rho(\tau_1) \dots \rho(\tau_n) R(b) \delta\left(\sum_{i=1}^n \tau_i + b - t\right). \quad (2.18)$$

In Laplace space, it is readily found that [24]

$$\mathcal{L}_t \langle \tau_t \rangle = \frac{1}{s} \int_0^\infty d\tau \tau \rho(\tau) e^{-s\tau} = -\frac{1}{s} \frac{d\hat{\rho}(s)}{ds}. \quad (2.19)$$

2.4 Asymptotic distribution of the time of the n th renewal

As can be seen on (2.7), the two quantities N_t and t_n represent complementary facets of a renewal process. In particular the asymptotic behaviours of these quantities in the long-time regime go hand in hand. We start by discussing the simpler case of t_n , before delving in that of N_t in the next section.

As we now show, when the number n of time intervals becomes large, the asymptotic growth of t_n obeys the following dichotomy, dictated by the law of large numbers.

Finite $\langle \tau \rangle$

In this case, i.e., for $\theta > 1$, we have

$$\langle t_n \rangle = n \langle \tau \rangle. \quad (2.20)$$

According to the law of large numbers, $t_n/n \rightarrow \langle \tau \rangle$ when $n \rightarrow \infty$, in probability. This essentially means that typical fluctuations of t_n around its mean value grow less rapidly than linearly in n . These fluctuations are therefore subextensive, i.e., relatively negligible. They can be characterised more precisely as follows. If $\text{Var } \tau = \langle \tau^2 \rangle - \langle \tau \rangle^2$ is finite, i.e., for $\theta > 2$, then

$$\text{Var } t_n = n \text{Var } \tau.$$

According to the central limit theorem, the difference $t_n - n \langle \tau \rangle$ grows as \sqrt{n} , and has an asymptotic normal distribution. If, on the other hand, $\text{Var } \tau$ is divergent, i.e., for $1 < \theta < 2$, the difference $t_n - n \langle \tau \rangle$ grows as $n^{1/\theta}$, and its asymptotic distribution is a Lévy stable law.

Divergent $\langle \tau \rangle$

In this case, i.e., for $\theta < 1$, the law of large numbers does not apply. The sum t_n grows more rapidly than linearly in n and keeps fluctuating. Using (2.4) and (2.8), we have indeed

$$\langle e^{-st_n} \rangle = \hat{\rho}(s)^n \approx e^{-nas^\theta},$$

and therefore (see (2.5))

$$t_n \approx (an)^{1/\theta} L_\theta = \tau_0 (\Gamma(1 - \theta) n)^{1/\theta} L_\theta, \quad (2.21)$$

where the rescaled random variable L_θ is distributed according to the normalised one-sided Lévy stable law of index θ , with density

$$f_{L_\theta}(x) = \int \frac{ds}{2\pi i} e^{sx-s^\theta} \quad (0 < x < +\infty). \quad (2.22)$$

The power-law tail

$$f_{L_\theta}(x) \approx \frac{\theta}{\Gamma(1-\theta) x^{1+\theta}}$$

mirrors that of the underlying density $\rho(\tau)$.

Marginal situation

When $\theta = 1$, the first moment $\langle \tau \rangle$ diverges logarithmically, thus the law of large numbers is affected by logarithmic corrections. Using (2.6), we have indeed

$$\langle e^{-st_n} \rangle \approx e^{n\tau_0 s \ln(\tau_* s)},$$

and therefore

$$t_n \approx n\tau_0 \left(\ln \frac{n\tau_0}{\tau_*} + \Xi \right). \quad (2.23)$$

The expression between the parentheses is the sum of a deterministic component, which grows logarithmically with n , and of a finite fluctuating part Ξ , following a Landau distribution [27],

$$f_\Xi(\xi) = \int \frac{dz}{2\pi i} e^{z\xi + z \ln z} \quad (-\infty < \xi < +\infty). \quad (2.24)$$

The right tail of this distribution,

$$f_\Xi(\xi) \approx \frac{1}{\xi^2} \quad (\xi \rightarrow +\infty),$$

mirrors that of the underlying density $\rho(\tau)$, and implies that $\langle \Xi \rangle$ is logarithmically divergent.

2.5 Asymptotic distribution of the number N_t of renewals

The results summarised below highlight the close connection between the statistics of the sum t_n of the first n time intervals for a fixed large number n of intervals, and of the number N_t of renewals up to a fixed large observation time t . In particular, the dichotomy between finite and infinite mean $\langle \tau \rangle$, described in section 2.4, also prevails for the asymptotic distribution of N_t (see, e.g., [2,24]).

Finite $\langle \tau \rangle$

In this case, i.e., for $\theta > 1$, the analysis of (2.16) and (2.17) shows that the mean number of events scales as

$$\langle N_t \rangle \approx \frac{t}{\langle \tau \rangle}, \quad (2.25)$$

and N_t exhibits subextensive, i.e., relatively negligible, fluctuations around this mean value. The two ensembles defined above are therefore equivalent, in the sense used in thermodynamics. In other words, time and the number of events are asymptotically proportional to each other, as testified by (2.20) and (2.25). Furthermore, these quantities are tightly related, in the sense that the relative fluctuations between the two quantities are negligible.

The fluctuations of N_t can be characterised more precisely as follows. If $\text{Var } \tau$ is finite, i.e., for $\theta > 2$, we have

$$\text{Var } N_t \approx \frac{\text{Var } \tau}{\langle \tau \rangle^3} t.$$

The difference $N_t - t/\langle \tau \rangle$ grows as \sqrt{t} , and has an asymptotic normal distribution. If $\text{Var } \tau$ is divergent, i.e., for $1 < \theta < 2$, the difference $N_t - t/\langle \tau \rangle$ grows as $t^{1/\theta}$ and its asymptotic distribution is a Lévy stable law. To mention a further subtlety, the variance of N_t grows as $t^{3-\theta}$, with an exponent larger than the exponent $2/\theta$ describing typical square fluctuations. The exponent difference $3 - \theta - 2/\theta = (2 - \theta)(\theta - 1)/\theta$ is positive and vanishes both for $\theta \rightarrow 1$ and for $\theta \rightarrow 2$ [24].

Renewal processes with a finite mean time interval $\langle \tau \rangle$ become stationary in the regime of late times. One-time observables, such as the distribution of B_t or of the excess time $E_t = t_{N_t+1} - t$, reach well-defined limiting forms, whereas two-time quantities depend solely on the difference between the two times, asymptotically. For instance, the number of renewals between times t and $t + t'$ only depends on the time separation t' , when t is large [24].

Divergent $\langle \tau \rangle$

In this case, i.e., for $\theta < 1$, the number N_t of events grows sublinearly with time and keeps fluctuating. Its mean value can be obtained from (2.4), (2.16), yielding

$$\langle N_t \rangle \approx \frac{\sin \pi \theta}{\pi \theta} \left(\frac{t}{\tau_0} \right)^\theta. \quad (2.26)$$

Moreover, its full distribution can be derived from (2.12), which translates to

$$\hat{p}_n(s) \approx a s^{\theta-1} e^{-nas^\theta}. \quad (2.27)$$

Thus, setting

$$N_t \approx X_\theta \frac{t^\theta}{a} = \frac{X_\theta}{\Gamma(1-\theta)} \left(\frac{t}{\tau_0} \right)^\theta, \quad (2.28)$$

we find that the probability density of the rescaled random variable X_θ is

$$f_{X_\theta}(x) = \int \frac{dz}{2\pi i} z^{\theta-1} e^{z-xz^\theta} \quad (x > 0), \quad (2.29)$$

which entails that the random variable X_θ can be written as [28, 29]

$$X_\theta = L_\theta^{-\theta}, \quad (2.30)$$

where the distribution of L_θ is the Lévy stable law (2.22). This manifests the equivalence of (2.21) and (2.28), under the replacement of N_t by n , and t_n by t : in the two ensembles defined above, the number of events scales as a power of time with exponent θ . However, at variance with the situation where $\langle \tau \rangle$ is finite, the asymptotic relations (2.21) and (2.28) between time and the number of events involve a fluctuating variable, denoted by L_θ or X_θ , respectively.

Renewal processes with a divergent $\langle \tau \rangle$ exhibit self-similar behaviour and universality at late times. In particular, dimensionless observables such as the ratios B_t/t and E_t/t , as well as the rescaled occupation time, have non-trivial limiting distributions, that depend solely on the exponent θ . Furthermore, the non-stationarity of the processes imply that two-time quantities depend on both instances of time, asymptotically. For instance, the number of renewals between times t and $t + t'$ now depends on both the waiting time t and the time separation t' , a property referred to as aging [24].

We also provide, for future reference, several results pertaining to the density $f_{X_\theta}(x)$ of the rescaled random variable X_θ . The integral representation (2.29) implies that $f_{X_\theta}(x)$ is regular at small x :

$$f_{X_\theta}(x) = \frac{1}{\Gamma(1-\theta)} - \frac{x}{\Gamma(1-2\theta)} + \dots \quad (2.31)$$

A saddle-point treatment shows that this density decays as a compressed exponential at large x , for all $0 < \theta < 1$, according to

$$f_{X_\theta}(x) \sim \exp\left(- (1-\theta)(\theta^\theta x)^{1/(1-\theta)}\right). \quad (2.32)$$

This fast decay has two consequences. First, all the moments of X_θ are finite. They are given by the explicit formula

$$\langle X_\theta^k \rangle = \frac{k!}{\Gamma(k\theta + 1)}. \quad (2.33)$$

Second, the corresponding Laplace transform $\hat{f}_{X_\theta}(u)$ is an entire function in the whole u -plane. This reads explicitly [2, 28]

$$\hat{f}_{X_\theta}(u) = \int_0^\infty dx e^{-ux} f_{X_\theta}(x) = \sum_{k \geq 0} \frac{(-u)^k}{\Gamma(k\theta + 1)} = \mathbb{E}_\theta(-u), \quad (2.34)$$

where $\mathbb{E}_\theta(z)$ is the Mittag-Leffler function of index θ (see [30] for a review)⁵.

Figure 3 shows plots of the density $f_{X_\theta}(x)$ for several values of the index θ (see legend). This distribution is a monotonically decreasing function of x for $\theta < 1/2$, whereas it exhibits a non-trivial maximum for $1/2 < \theta < 1$.

For $\theta \rightarrow 0$, the distribution of X_θ becomes a simple exponential, with density

$$f_{X_0}(x) = e^{-x}, \quad \hat{f}_{X_0}(u) = \frac{1}{1+u}.$$

For $\theta = 1/2$, the distribution of X_θ is a half-Gaussian, with density

$$f_{X_{1/2}}(x) = \frac{e^{-x^2/4}}{\sqrt{\pi}}, \quad \hat{f}_{X_{1/2}}(u) = e^{u^2} \operatorname{erfc} u, \quad (2.35)$$

where erfc is the complementary error function.

For $\theta \rightarrow 1$, the distribution of X_θ becomes degenerate:

$$f_{X_1}(x) = \delta(x-1), \quad \hat{f}_{X_1}(u) = e^{-u}. \quad (2.36)$$

Marginal situation

When $\theta = 1$, the first moment $\langle \tau \rangle$ diverges logarithmically and the above results are affected by logarithmic corrections. Let us focus on the mean number N_t of events. Inserting the asymptotic expression (2.6) of $\hat{\rho}(s)$ into (2.16), we obtain

$$\mathcal{L}_t \langle N_t \rangle \approx -\frac{1}{\tau_0 s^2 \ln(\tau_* s)},$$

hence

$$\langle N_t \rangle \approx \frac{1}{\ln(t/\tau_*) + \gamma - 1} \frac{t}{\tau_0}, \quad (2.37)$$

⁵ The distribution of the random variable X_θ is named Mittag-Leffler by some authors [31]. Another definition of the Mittag-Leffler distribution is used in other works, though (see, e.g., [32]).

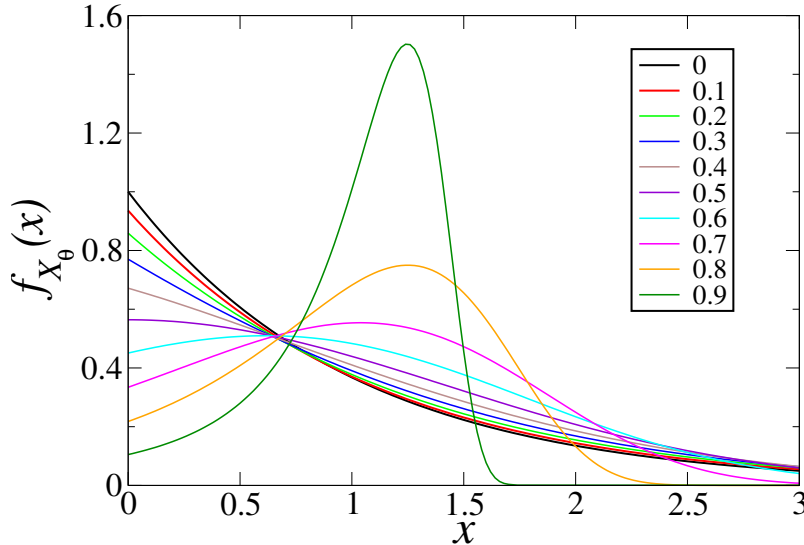


Fig. 3 Probability density $f_{X_\theta}(x)$ of the rescaled random variable X_θ entering (2.28), for several values of the index θ (see legend).

where γ is Euler's constant.

Typical fluctuations of N_t around its mean value are again relatively negligible, albeit marginally, as their typical size is smaller than $\langle N_t \rangle$ by one power of $\ln(t/\tau_*)$. Skipping details, let us mention the formula

$$N_t \approx \frac{1}{\ln(t/\tau_*) + \Xi} \frac{t}{\tau_0}, \quad (2.38)$$

where the random variable Ξ has the Landau distribution (2.24). A comparison between (2.23) and (2.38) again demonstrates a tight match between the two aforementioned ensembles. Note however that there is no simple connection between (2.37) and (2.38), as $\langle \Xi \rangle$ is divergent.

2.6 Asymptotic behaviour of the mean of the single-interval distribution

The asymptotic analysis of the quantity defined in (2.18) can be done along the same lines as above, using (2.19), and leads to the following results.

If, first, $\langle \tau \rangle$ is finite, i.e., $\theta > 1$, then $\langle \tau_t \rangle$ converges to $\langle \tau \rangle$, in line with (2.25). On the other hand, if $\langle \tau \rangle$ is divergent, i.e., $\theta < 1$, we have

$$\langle \tau_t \rangle \approx \frac{\theta \tau_0^\theta}{1 - \theta} t^{1-\theta}. \quad (2.39)$$

The product of this quantity by the mean number of events (see (2.26)),

$$\langle N_t \rangle \langle \tau_t \rangle \approx \frac{\sin \pi \theta}{\pi(1 - \theta)} t,$$

grows linearly in time, with a universal amplitude depending only on the exponent θ . In the marginal situation where $\theta = 1$, substituting (2.6) in (2.19) yields

$$\mathcal{L}_t \langle \tau_t \rangle \approx -\frac{\tau_0}{s} (\ln(\tau_* s) + 1),$$

hence

$$\langle \tau_t \rangle \approx \tau_0 \left(\ln \frac{t}{\tau_\star} + \gamma - 1 \right). \quad (2.40)$$

Thus, interestingly, (2.37) can be rewritten as

$$\langle N_t \rangle \approx \frac{t}{\langle \tau_t \rangle}.$$

More precisely,

$$\langle N_t \rangle \langle \tau_t \rangle = \left(1 + O\left(\frac{1}{(\ln t)^2} \right) \right) t.$$

3 Two nested renewal processes: definition and general results

As depicted in figure 1, the stochastic process under study is obtained by the replication of a renewal process, defined by the sequence τ_1, τ_2, \dots of iid random intervals of time, with common probability density $\rho(\tau)$ —the *internal renewal process*—according to another renewal process, defined by the sequence $\mathbf{T}_1, \mathbf{T}_2, \dots$ of iid random intervals of time, with common probability density $f(T)$ —the *external renewal process*. Events separated by the time intervals τ_1, τ_2, \dots , shown as crosses in figure 1, are referred to as internal events, whereas events separated by the time intervals $\mathbf{T}_1, \mathbf{T}_2, \dots$, shown as dots, are referred to as external events. We shall alternatively refer to external events as resetting events, since the process defined in this manner can also be interpreted as a renewal process, characterised by the density $\rho(\tau)$, that is reset at random time intervals, drawn from the density $f(T)$.

In the following, our objective is to analyse the stochastic process made of these two nested renewal processes, with a focus on the statistics of the number \mathcal{N}_t of internal events occurring up to time t . We shall be mostly interested in the case where the two probability densities of the internal and external processes have power-law decays of the form

$$\rho(\tau) \approx \frac{\theta_1 \tau_0^{\theta_1}}{\tau^{1+\theta_1}}, \quad f(T) \approx \frac{\theta_2 T_0^{\theta_2}}{T^{1+\theta_2}}, \quad (3.1)$$

with arbitrary positive exponents θ_1, θ_2 . As mentioned earlier, thin-tailed distributions with finite moments of all orders formally correspond to taking infinite values for these exponents.

The number of resetting events, i.e., of time intervals $\mathbf{T}_1, \mathbf{T}_2, \dots$, up to time t is denoted by M_t . These intervals obey the sum rule

$$\mathbf{T}_1 + \mathbf{T}_2 + \dots + \mathbf{T}_{M_t} + B_t = t, \quad (3.2)$$

where the backward recurrence time B_t is, as previously defined, the time elapsed since the last resetting event. Within each interval \mathbf{T}_i , there are $N_{\mathbf{T}_i}$ internal events induced by $\rho(\tau)$. The total number of these internal events up to time t is given by

$$\mathcal{N}_t = N_{\mathbf{T}_1} + N_{\mathbf{T}_2} + \dots + N_{\mathbf{T}_{M_t}} + N_{B_t}. \quad (3.3)$$

In this expression, $N_{\mathbf{T}_1}, N_{\mathbf{T}_2}, \dots$ are doubly stochastic quantities, to be distinguished from N_{T_1}, N_{T_2}, \dots , since the time variables $\mathbf{T}_1, \mathbf{T}_2, \dots$ are random variables themselves. The former are averaged over both internal and external processes, the latter on the internal process only (see (4.1)).

All information on the distribution of \mathcal{N}_t is encoded in the generating function

$$\mathcal{Z}(z, t) = \langle z^{\mathcal{N}_t} \rangle,$$

where the average is taken over the realisations $\mathcal{C} = \{T_1, T_2, \dots, B\}$ of the external variables $\mathbf{T}_1, \mathbf{T}_2, \dots, B_t$, with the weight (for fixed $M_t = \nu$)

$$P(\mathcal{C}) = f(T_1) \dots f(T_\nu) \Phi(B) \delta\left(\sum_{i=1}^{\nu} T_i + B - t\right), \quad (3.4)$$

where

$$\Phi(B) = \mathbb{P}(\mathbf{T} > B) = \int_B^{\infty} dT f(T)$$

is the survival probability of the external process, and over the realisations $\tilde{\mathcal{C}} = \{\tau_1, \tau_2, \dots, b\}$ of the internal variables, $\tau_1, \tau_2, \dots, b_T$, attached to each interval $\mathbf{T}_1, \mathbf{T}_2, \dots$, with the weight (for fixed $N_T = n$)

$$P(\tilde{\mathcal{C}}) = \rho(\tau_1) \dots \rho(\tau_n) R(b) \delta\left(\sum_{i=1}^n \tau_i + b - T\right).$$

Thus

$$\mathcal{Z}(z, t) = \sum_{\mathcal{C}} P(\mathcal{C}) \sum_{\tilde{\mathcal{C}}_1, \tilde{\mathcal{C}}_2, \dots} P(\tilde{\mathcal{C}}_1) z^{N_{T_1}} P(\tilde{\mathcal{C}}_2) z^{N_{T_2}} \dots,$$

with the notations

$$\sum_{\mathcal{C}} = \sum_{\nu \geq 0} \int_0^{\infty} dT_1 \dots dT_\nu dB, \quad \sum_{\tilde{\mathcal{C}}} = \sum_{n \geq 0} \int_0^{\infty} d\tau_1 \dots d\tau_n db.$$

The average over the internal variables of each term $z^{N_{T_i}}$ with the weight $P(\tilde{\mathcal{C}})$ gives a factor $Z(z, T_i)$ (see (2.14)). We then average over the external variables with the weight $P(\mathcal{C})$ to obtain

$$\mathcal{Z}(z, t) = \sum_{\mathcal{C}} P(\mathcal{C}) Z(z, T_1) \dots Z(z, T_\nu) Z(z, B). \quad (3.5)$$

This expression is a convolution, which is easier to handle in Laplace space, leading to

$$\hat{\mathcal{Z}}(z, s) = \mathcal{L}_t \mathcal{Z}(z, t) = \sum_{\nu \geq 0} \int_0^{\infty} dT_1 e^{-sT_1} f(T_1) Z(z, T_1) \dots \int_0^{\infty} dB e^{-sB} \Phi(B) Z(z, B) \quad (3.6)$$

with

$$\hat{\varphi}(z, s) = \int_0^{\infty} dT e^{-sT} f(T) Z(z, T), \quad (3.7)$$

$$\hat{\psi}(z, s) = \int_0^{\infty} dT e^{-sT} \Phi(T) Z(z, T), \quad (3.8)$$

thus finally

$$\hat{\mathcal{Z}}(z, s) = \frac{\hat{\psi}(z, s)}{1 - \hat{\varphi}(z, s)}. \quad (3.9)$$

This key equation is the starting point of all forthcoming developments.

Expressions for the moments $\langle \mathcal{N}_t^k \rangle$ in Laplace space can be obtained by differentiating (3.9) with respect to z at $z = 1$, along the lines of (2.16). We thus obtain

$$\mathcal{L}_t \langle \mathcal{N}_t \rangle = \frac{I_1(s)}{s(1 - \hat{f}(s))} + \frac{I_2(s)}{1 - \hat{f}(s)}, \quad (3.10)$$

$$\mathcal{L}_t \langle \mathcal{N}_t^2 \rangle = \frac{I_1(s) + sI_2(s) + I_3(s) + sI_4(s)}{s(1 - \hat{f}(s))} + \frac{2I_1(s)(I_1(s) + sI_2(s))}{s(1 - \hat{f}(s))^2}, \quad (3.11)$$

with the definitions

$$\begin{aligned} I_1(s) &= \int_0^\infty dT e^{-sT} f(T) \langle N_T \rangle, & I_2(s) &= \int_0^\infty dT e^{-sT} \Phi(T) \langle N_T \rangle, \\ I_3(s) &= \int_0^\infty dT e^{-sT} f(T) \langle N_T^2 \rangle, & I_4(s) &= \int_0^\infty dT e^{-sT} \Phi(T) \langle N_T^2 \rangle. \end{aligned} \quad (3.12)$$

Let us note, for later reference (see section 8), that, by applying the same reasoning, we can obtain the expression of $\langle z^{N_{B_t}} \rangle$ in Laplace space. Indeed, we have (see (3.5))

$$\langle z^{N_{B_t}} \rangle = \sum_{\mathcal{C}} P(\mathcal{C}) Z(z, B),$$

hence (see (3.6))

$$\mathcal{L}_t \langle z^{N_{B_t}} \rangle = \frac{\hat{\psi}(z, s)}{1 - \hat{f}(s)}. \quad (3.13)$$

It follows that

$$\mathcal{L}_t \mathbb{P}(N_{B_t} = n) = \frac{\int_0^\infty dT e^{-sT} \Phi(T) p_n(T)}{1 - \hat{f}(s)}, \quad (3.14)$$

and therefore

$$\mathcal{L}_t \langle N_{B_t}^k \rangle = \frac{\int_0^\infty dT e^{-sT} \Phi(T) \langle N_T^k \rangle}{1 - \hat{f}(s)}. \quad (3.15)$$

In particular,

$$\mathcal{L}_t \langle N_{B_t} \rangle = \frac{I_2(s)}{1 - \hat{f}(s)}, \quad (3.16)$$

which is the second term on the right-hand side of (3.10). Accordingly, the first term on the right-hand side of the latter equation represents the Laplace transform of the mean sum of the first M_t terms in (3.3).

4 Phase diagram

The asymptotic behaviour of the number \mathcal{N}_t of internal events in the long-time regime is determined by the characteristics of the underlying probability densities $\rho(\tau)$ and $f(T)$, and chiefly by their tail exponents θ_1 and θ_2 . The subsequent analysis evidences four regions, labelled in order of increasing complexity, and depicted in the phase diagram presented in figure 2. The behaviour of \mathcal{N}_t along the boundaries between these regions is considered at the end of this section.

Region A ($\theta_2 > 1$)

When the first moment $\langle T \rangle$ of the external density $f(T)$ is finite, that is, if $\theta_2 > 1$, the first term in the right-hand side of (3.10) gives the leading contribution as $s \rightarrow 0$ (see section 8 for an analysis of the second term). The integral $I_1(s)$ defined in (3.12) has a finite limit for $s \rightarrow 0$, which represents the mean number $\langle N_{\mathbf{T}} \rangle$ of internal events in the random interval $(0, \mathbf{T})$ [3, 33], i.e.,

$$I_1(0) = \langle N_{\mathbf{T}} \rangle = \int_0^\infty dT f(T) \langle N_T \rangle = \left\langle \sum_{n \geq 0} n p_n(\mathbf{T}) \right\rangle, \quad (4.1)$$

where the average in the rightmost expression pertains to the random variable \mathbf{T} . The denominator of the first term in the right-hand side of (3.10) behaves as $\langle \mathbf{T} \rangle s^2$, thus, finally,

$$\langle \mathcal{N}_t \rangle \approx \frac{\langle N_{\mathbf{T}} \rangle}{\langle \mathbf{T} \rangle} t. \quad (4.2)$$

The interpretation of this result is intuitively clear: asymptotically, $\langle \mathcal{N}_t \rangle$ is the product of the mean number $\langle N_{\mathbf{T}} \rangle$ of internal events between two resettings by the mean number of resettings in $(0, t)$ (see (2.25)),

$$\langle \mathcal{N}_t \rangle \approx \langle N_{\mathbf{T}} \rangle \langle M_t \rangle. \quad (4.3)$$

Similarly, the square of $I_1(0)$ gives the leading contribution to (3.11) as $s \rightarrow 0$. We thus obtain the estimate

$$\langle \mathcal{N}_t^2 \rangle \approx \frac{\langle N_{\mathbf{T}} \rangle^2}{\langle \mathbf{T} \rangle^2} t^2 \approx \langle N_{\mathbf{T}} \rangle^2 \langle M_t \rangle^2,$$

demonstrating that typical fluctuations of \mathcal{N}_t around its mean value (4.2) are relatively negligible.

Region B ($\theta_2 < 1 < \theta_1$)

In this region, since $\theta_2 < 1$, the first moment of the external density $f(T)$ is divergent. In the present context, (2.2), (2.3), (2.4) and (2.5) become

$$f(T) \approx \frac{\theta_2 T_0^{\theta_2}}{T^{1+\theta_2}}, \quad \Phi(T) \approx \frac{T_0^{\theta_2}}{T^{\theta_2}}, \quad (4.4)$$

$$1 - \hat{f}(s) \approx a_2 s^{\theta_2}, \quad a_2 = \Gamma(1 - \theta_2) T_0^{\theta_2}. \quad (4.5)$$

The integrals $I_1(s)$ and $I_2(s)$ are divergent for $s \rightarrow 0$, and their leading behaviour can be estimated by using $\langle N_T \rangle \approx T / \langle \tau \rangle$. We thus obtain

$$I_1(s) + s I_2(s) \approx \frac{a_2}{\langle \tau \rangle} s^{\theta_2 - 1},$$

where both integrals contribute to the above estimate, hence

$$\mathcal{L}_t \langle \mathcal{N}_t \rangle \approx \frac{1}{\langle \tau \rangle s^2},$$

and finally

$$\langle \mathcal{N}_t \rangle \approx \frac{t}{\langle \tau \rangle}. \quad (4.6)$$

The integrals $I_3(s)$ and $I_4(s)$ are also divergent as $s \rightarrow 0$. Some algebra yields the estimate

$$\langle \mathcal{N}_t^2 \rangle \approx \frac{t^2}{\langle \tau \rangle^2},$$

showing that typical fluctuations of \mathcal{N}_t around its mean value are again relatively negligible. To conclude, asymptotically, the internal process is not influenced by the external one, as far as the mean $\langle \mathcal{N}_t \rangle$ is concerned.

Region C ($\theta_1 < \theta_2 < 1$)

In this region, both exponents are less than unity, which implies that large fluctuations in the statistics of \mathcal{N}_t are to be expected. Since $\theta_1 < \theta_2$, it is also expected that the number of internal events between any two consecutive resettings is typically finite and of the order of $\langle N_{\mathbf{T}} \rangle$. This is corroborated by the fact that the expression (4.1) for $I_1(0)$ is convergent for $\theta_1 < \theta_2$. Using the estimate (4.5) for $1 - \hat{f}(s)$ in (3.10), we obtain

$$\langle \mathcal{N}_t \rangle \approx \langle N_{\mathbf{T}} \rangle \frac{\sin \pi \theta_2}{\pi \theta_2} \left(\frac{t}{T_0} \right)^{\theta_2}. \quad (4.7)$$

As in region A, $\langle \mathcal{N}_t \rangle$ has the form (4.3), i.e., it is asymptotically the product of the mean number $\langle N_{\mathbf{T}} \rangle$ of internal events between two resettings by the mean number of resettings in $(0, t)$, given in the present case by (2.26).

This product structure extends to the entire asymptotic distribution of \mathcal{N}_t . This can be shown by estimating (3.9) as follows. Anticipating that typical values of \mathcal{N}_t will be large, we set $z = e^{-p}$, and analyse the regime where p is small. To leading order as $p \rightarrow 0$, the numerator $\hat{\psi}(z, s)$ can be replaced by

$$\hat{\psi}(1, s) = \hat{\Phi}(s) = \frac{1 - \hat{f}(s)}{s} \approx a_2 s^{\theta_2 - 1}.$$

The analysis of the denominator of (3.9) requires some care. We have

$$\begin{aligned} 1 - \hat{\varphi}(z, s) &= \int_0^\infty dT f(T) (1 - e^{-sT} Z(z, T)) \\ &\approx \int_0^\infty dT f(T) (1 - e^{-sT} + p \langle N_{\mathbf{T}} \rangle) \\ &\approx 1 - \hat{f}(s) + p \langle N_{\mathbf{T}} \rangle \\ &\approx a_2 s^{\theta_2} + p \langle N_{\mathbf{T}} \rangle, \end{aligned}$$

where we used the expansion $Z(z, T) = 1 - p \langle N_{\mathbf{T}} \rangle + \dots$. Finally, (3.9) reduces to

$$\mathcal{L}_t \langle e^{-p \mathcal{N}_t} \rangle \approx \frac{a_2 s^{\theta_2 - 1}}{a_2 s^{\theta_2} + p \langle N_{\mathbf{T}} \rangle},$$

yielding for the distribution of \mathcal{N}_t in the continuum limit

$$\mathcal{L}_t f_{\mathcal{N}_t}(n) \approx \frac{a_2 s^{\theta_2 - 1}}{\langle N_{\mathbf{T}} \rangle} \exp\left(-\frac{n a_2 s^{\theta_2}}{\langle N_{\mathbf{T}} \rangle}\right).$$

Comparing this expression to (2.27), we obtain the scaling result

$$\mathcal{N}_t \approx \langle N_{\mathbf{T}} \rangle \frac{X_{\theta_2}}{\Gamma(1 - \theta_2)} \left(\frac{t}{T_0} \right)^{\theta_2} \approx \langle N_{\mathbf{T}} \rangle M_t, \quad (4.8)$$

where the rescaled random variable X_{θ_2} has density $f_{X_{\theta_2}}(x)$, given by (2.29). This expression, which generalises (4.7), shows that \mathcal{N}_t is, asymptotically, equal to the product of the mean number $\langle N_{\mathbf{T}} \rangle$ of internal events between two resettings by the random number of resettings (see (2.28)).

Region D ($\theta_2 < \theta_1 < 1$)

In this region, the statistics of \mathcal{N}_t is more complex. First, since both exponents are less than unity, large fluctuations in \mathcal{N}_t are to be expected. Second, the number of internal events between any two consecutive resettings is itself expected to diverge for late times. The integrals $I_1(s)$ and $I_2(s)$ are indeed divergent as $s \rightarrow 0$. Their leading behaviour can be estimated by using the expression (2.26) of $\langle N_T \rangle$, where θ is replaced by θ_1 . We thus obtain

$$I_1(s) + sI_2(s) \approx \frac{\sin \pi \theta_1}{\pi \theta_1} \frac{T_0^{\theta_2}}{\tau_0^{\theta_1}} \Gamma(\theta_1 - \theta_2) s^{\theta_2 - \theta_1}.$$

Substituting this expression and the estimate (4.5) for $1 - \hat{f}(s)$ into (3.10), we obtain

$$\langle \mathcal{N}_t \rangle \approx E_{\theta_1, \theta_2} \frac{\sin \pi \theta_1}{\pi \theta_1} \left(\frac{t}{\tau_0} \right)^{\theta_1}, \quad E_{\theta_1, \theta_2} = \frac{\Gamma(\theta_1 - \theta_2)}{\Gamma(\theta_1) \Gamma(1 - \theta_2)}, \quad (4.9)$$

which is the product of the enhancement factor E_{θ_1, θ_2} by the mean number of events of the internal process in the absence of resetting (see (2.26)). The enhancement factor becomes unity as $\theta_2 \rightarrow 0$, in which case (4.9) gives back (2.26), where θ is replaced by θ_1 . This factor is an increasing function of θ_2 , which diverges as $\theta_2 \rightarrow \theta_1$ (see section 5.5 for further discussion on these two limits).

The presence of the enhancement factor E_{θ_1, θ_2} , which depends continuously on the two exponents θ_1 and θ_2 , confirms that region D is where the distribution of \mathcal{N}_t exhibits the highest level of complexity. The analysis of the entire asymptotic distribution of \mathcal{N}_t in this region is the focus of section 5.

We conclude this section by examining the behaviour of \mathcal{N}_t along the boundaries between the various regions of the phase diagram shown in figure 2, in order of increasing complexity.

Between regions A and B ($\theta_2 = 1$ and $\theta_1 > 1$)

If θ_2 goes to unity from region A, both $\langle N_T \rangle$ and $\langle T \rangle$ diverge at the same pace, and their ratio goes to the finite limit $1/\langle \tau \rangle$, hence the expressions (4.2) and (4.6) match smoothly.

Between regions A and C ($\theta_2 = 1$ and $0 < \theta_1 < 1$)

Along this phase boundary, $\langle N_T \rangle$ is convergent, and $\hat{f}(s) \approx 1 + T_0 s \ln(T_* s)$, in analogy with (2.6). Inserting these estimates into (3.10), we obtain

$$\mathcal{L}_t \langle \mathcal{N}_t \rangle \approx - \frac{\langle N_T \rangle}{T_0 s^2 \ln(T_* s)},$$

hence

$$\langle \mathcal{N}_t \rangle \approx \frac{\langle N_T \rangle}{\ln(t/T_*) + \gamma - 1} \frac{t}{T_0}.$$

This can be rewritten as (see (2.40))

$$\langle \mathcal{N}_t \rangle \approx \frac{\langle N_T \rangle}{\langle T_t \rangle} t,$$

which matches with (4.2). One can verify that typical fluctuations of \mathcal{N}_t around its mean value are marginally negligible. This property, which holds all over region A, is emerging in region C as well in the limit $\theta_2 \rightarrow 1$ (see (2.36)).

Between regions B and D ($\theta_1 = 1$ and $0 < \theta_2 < 1$)

Along this phase boundary, the integrals $I_1(s)$ and $I_2(s)$ are divergent as $s \rightarrow 0$. Their leading behaviour can be estimated by inserting the expression (2.37) of $\langle N_T \rangle$ into (3.12). We thus obtain

$$I_1(s) + sI_2(s) \approx -\frac{T_0^{\theta_2} \Gamma(1 - \theta_2)}{\tau_0 s^{1-\theta_2} \ln(\tau_* s)}.$$

Substituting this expression and the estimate (4.5) for $1 - \hat{f}(s)$ into (3.10), we obtain

$$\mathcal{L}_t \langle \mathcal{N}_t \rangle \approx -\frac{1}{\tau_0 s^2 \ln(\tau_* s)},$$

hence

$$\langle \mathcal{N}_t \rangle \approx \frac{1}{\ln(t/\tau_*) + \gamma - 1} \frac{t}{\tau_0},$$

thus (see (2.40))

$$\langle \mathcal{N}_t \rangle \approx \frac{t}{\langle \tau_t \rangle},$$

which matches with (4.6).

Typical fluctuations of \mathcal{N}_t around its mean are again marginally negligible. This property, which holds all over region B, is emerging in region D as well in the limit $\theta_1 \rightarrow 1$ (see (5.30)).

Between regions C and D ($0 < \theta_1 = \theta_2 < 1$)

Along this phase boundary, the integral $I_1(s)$ is logarithmically divergent, whereas $I_2(s)$ can be neglected. Denoting by θ the common value of θ_1 and θ_2 , and inserting the expressions (2.26) and (3.1) into (3.12), we obtain

$$\mathcal{L}_t \langle \mathcal{N}_t \rangle \approx -\frac{\sin \pi \theta}{\pi \Gamma(1 - \theta) \tau_0^\theta} \frac{\ln s}{s^{1+\theta}},$$

where the finite part of the logarithm has no simple expression in general and will therefore be omitted. This yields

$$\langle \mathcal{N}_t \rangle \approx \frac{\sin^2 \pi \theta}{\pi^2 \theta} \left(\frac{t}{\tau_0} \right)^\theta \ln t. \quad (4.10)$$

At variance with all other phase boundaries, the number \mathcal{N}_t of internal events keeps fluctuating in the present situation. It is indeed clear that \mathcal{N}_t is proportional to the reduced random variable X_θ as the phase boundary is approached from either side. This property, which holds all over region C, is emerging in region D as well in the limit $\theta_2 \rightarrow \theta_1$ (see (5.32)). The proportionality constant between \mathcal{N}_t and X_θ is determined by comparing the expressions (4.10) of $\langle \mathcal{N}_t \rangle$ and (2.33) of $\langle X_\theta \rangle$. We thus obtain the asymptotic estimate

$$\mathcal{N}_t \approx \frac{\sin \pi \theta}{\pi} \frac{X_\theta}{\Gamma(1 - \theta)} \left(\frac{t}{\tau_0} \right)^\theta \ln t$$

along the boundary between regions C and D.

The quadruple point ($\theta_1 = \theta_2 = 1$)

Skipping every detail, we mention that the mean number of internal events scales as

$$\langle \mathcal{N}_t \rangle \approx \frac{\ln \ln t}{\ln t} \frac{t}{\tau_0}$$

at the quadruple point where the four regions of the phase diagram meet.

5 Asymptotic distribution of \mathcal{N}_t in region D ($0 < \theta_2 < \theta_1 < 1$)

The growth law (4.9) of the mean number $\langle \mathcal{N}_t \rangle$ of internal events in region D suggests to postulate the scaling form

$$\mathcal{N}_t \approx \frac{Y_{\theta_1, \theta_2}}{\Gamma(1 - \theta_1)} \left(\frac{t}{\tau_0} \right)^{\theta_1}, \quad (5.1)$$

in analogy with (2.28), where the rescaled random variable Y_{θ_1, θ_2} has a non-trivial universal distribution depending only on the two exponents θ_1 and θ_2 , whose density will be denoted by $f_{Y_{\theta_1, \theta_2}}(y)$. The current section is dedicated to a thorough examination of this probability density.

5.1 Fundamental integral equation

Our starting point is again the exact expression (3.9). As in section 4, anticipating that typical values of \mathcal{N}_t are large for late times, we set $z = e^{-p}$, and analyse the regime where p is small. The scaling form (2.28) of N_t implies that the generating function $Z(z, t)$ defined in (2.14) scales as

$$Z(z, t) \approx \hat{f}_{X_{\theta_1}}(u), \quad u = \frac{p}{\Gamma(1 - \theta_1)} \left(\frac{t}{\tau_0} \right)^{\theta_1} \quad (5.2)$$

(see (2.34)) in the regime where p is small and t is large.

Inserting the tail expressions (4.4) and the scaling form (5.2) into the expression (3.8) for $\hat{\psi}(z, s)$, and changing the integration variable from T to the corresponding rescaled variable u , we obtain the scaling form

$$\hat{\psi}(z, s) \approx T_0^{\theta_2} s^{\theta_2 - 1} I(\lambda), \quad (5.3)$$

where

$$\lambda = \tau_0 s \left(\frac{\Gamma(1 - \theta_1)}{p} \right)^{1/\theta_1} \quad (5.4)$$

and

$$I(\lambda) = \frac{\lambda^{1 - \theta_2}}{\theta_1} \int_0^\infty du e^{-\lambda u^{1/\theta_1}} u^{(1 - \theta_2)/\theta_1 - 1} \hat{f}_{X_{\theta_1}}(u). \quad (5.5)$$

Using the definition (3.7) of $\hat{\varphi}(z, s)$, the denominator of (3.9) can be written as

$$\begin{aligned} 1 - \hat{\varphi}(z, s) &= 1 - \int_0^\infty dT f(T) e^{-sT} Z(z, T) \\ &= 1 - \hat{f}(s) + \int_0^\infty dT f(T) e^{-sT} (1 - Z(z, T)). \end{aligned}$$

Using again (4.4) and (5.2), we obtain the scaling form

$$1 - \hat{\varphi}(z, s) \approx (T_0 s)^{\theta_2} K(\lambda), \quad (5.6)$$

with

$$K(\lambda) = \Gamma(1 - \theta_2) + \theta_2 J(\lambda), \quad (5.7)$$

and

$$J(\lambda) = \frac{\lambda^{-\theta_2}}{\theta_1} \int_0^\infty du e^{-\lambda u^{1/\theta_1}} u^{-1 - \theta_2/\theta_1} (1 - \hat{f}_{X_{\theta_1}}(u)). \quad (5.8)$$

Finally, inserting (5.3) and (5.6) into (3.9), we are left with the estimate

$$\hat{\mathcal{Z}}(z, s) \approx \frac{I(\lambda)}{s K(\lambda)}. \quad (5.9)$$

On the other hand, the postulated scaling law (5.1) yields

$$\hat{\mathcal{Z}}(z, s) \approx \int_0^\infty dt e^{-st} \int_0^\infty dy e^{-uy} f_{Y_{\theta_1, \theta_2}}(y), \quad (5.10)$$

where u is defined in (5.2). Using the rescaled variable λ introduced in (5.4), as well as $\mu = u^{1/\theta_1}$, whereby $st = \lambda\mu$, we have

$$\hat{\mathcal{Z}}(z, s) \approx \frac{\lambda}{s} \int_0^\infty d\mu e^{-\lambda\mu} \int_0^\infty dy e^{-\mu^{\theta_1} y} f_{Y_{\theta_1, \theta_2}}(y). \quad (5.11)$$

A comparison between (5.9) and (5.11) corroborates the scaling form (5.1) and yields an integral equation for the density $f_{Y_{\theta_1, \theta_2}}(y)$, of the form

$$\mathcal{L}(\lambda) = \mathcal{R}(\lambda), \quad (5.12)$$

with, on the left-hand side,

$$\mathcal{L}(\lambda) = \lambda \int_0^\infty d\mu e^{-\lambda\mu} \int_0^\infty dy e^{-\mu^{\theta_1} y} f_{Y_{\theta_1, \theta_2}}(y), \quad (5.13)$$

and, on the right-hand side,

$$\mathcal{R}(\lambda) = \frac{I(\lambda)}{K(\lambda)}. \quad (5.14)$$

The fundamental equation (5.12) is the starting point of the analysis that follows, where we successively investigate the moments of Y_{θ_1, θ_2} (section 5.2), the behaviour of its probability density $f_{Y_{\theta_1, \theta_2}}(y)$ at small and large y (sections 5.3 and 5.4), the three limiting situations corresponding to the edges of region D (section 5.5), a measure of the fluctuations (section 5.6), and finally an integral representation of $f_{Y_{\theta_1, \theta_2}}(y)$ (section 5.7).

5.2 Moments of Y_{θ_1, θ_2}

The moments of Y_{θ_1, θ_2} can be extracted from (5.12) as follows. Consider first its left-hand side $\mathcal{L}(\lambda)$ given by (5.13). Expanding the exponential in the innermost integral as a power series in μ^{θ_1} and performing the integrals, we can recast $\mathcal{L}(\lambda)$ as a power series in the variable

$$\zeta = -\lambda^{-\theta_1}, \quad (5.15)$$

reading

$$\mathcal{L}(\lambda) \equiv \tilde{\mathcal{L}}(\zeta) = \sum_{k \geq 0} \frac{\Gamma(k\theta_1 + 1)}{k!} \langle Y_{\theta_1, \theta_2}^k \rangle \zeta^k. \quad (5.16)$$

Similarly, by inserting the power series (2.34) for $\hat{f}_{X_{\theta_1}}(u)$ into (5.5) and (5.8) and performing the integrals, we obtain the following power series in ζ :

$$I(\lambda) \equiv \tilde{I}(\zeta) = \sum_{k \geq 0} \frac{\Gamma(k\theta_1 + 1 - \theta_2)}{\Gamma(k\theta_1 + 1)} \zeta^k, \quad (5.17)$$

$$K(\lambda) \equiv \tilde{K}(\zeta) = -\theta_2 \sum_{k \geq 0} \frac{\Gamma(k\theta_1 - \theta_2)}{\Gamma(k\theta_1 + 1)} \zeta^k. \quad (5.18)$$

The functions $\tilde{I}(\zeta)$ and $\tilde{K}(\zeta)$ are simple generalisations of the Wright function (see [34] and references therein). They are analytic in the complex ζ -plane cut along the positive real axis from 1 to ∞ . They are related by the differential identity

$$\tilde{I}(\zeta) = \tilde{K}(\zeta) - \frac{\theta_1}{\theta_2} \zeta \tilde{K}'(\zeta),$$

where the accent denotes a differentiation, entailing that (see (5.14))

$$\mathcal{R}(\lambda) \equiv \tilde{\mathcal{R}}(\zeta) = \frac{\tilde{I}(\zeta)}{\tilde{K}(\zeta)} = 1 - \frac{\theta_1}{\theta_2} \frac{\zeta \tilde{K}'(\zeta)}{\tilde{K}(\zeta)} \quad (5.19)$$

is nearly a logarithmic derivative.

By identifying the coefficients of successive powers of ζ in the power series $\tilde{\mathcal{L}}(\zeta)$ (see (5.16)) and $\tilde{\mathcal{R}}(\zeta)$ (see (5.17), (5.18), (5.19)), we obtain explicit expressions for the moments of Y_{θ_1, θ_2} , depending only on the exponents θ_1 and θ_2 :

$$\begin{aligned} \langle Y_{\theta_1, \theta_2} \rangle &= \frac{\theta_1 \Gamma(\theta_1 - \theta_2)}{\Gamma(\theta_1 + 1)^2 \Gamma(1 - \theta_2)}, \\ \langle Y_{\theta_1, \theta_2}^2 \rangle &= \frac{4\theta_1 \Gamma(2\theta_1 - \theta_2)}{\Gamma(2\theta_1 + 1)^2 \Gamma(1 - \theta_2)} \\ &\quad + \frac{2\theta_1 \theta_2 \Gamma(\theta_1 - \theta_2)^2}{\Gamma(\theta_1 + 1)^2 \Gamma(2\theta_1 + 1) \Gamma(1 - \theta_2)^2}, \\ \langle Y_{\theta_1, \theta_2}^3 \rangle &= \frac{18\theta_1 \Gamma(3\theta_1 - \theta_2)}{\Gamma(3\theta_1 + 1)^2 \Gamma(1 - \theta_2)} \\ &\quad + \frac{18\theta_1 \theta_2 \Gamma(\theta_1 - \theta_2) \Gamma(2\theta_1 - \theta_2)}{\Gamma(\theta_1 + 1) \Gamma(2\theta_1 + 1) \Gamma(3\theta_1 + 1) \Gamma(1 - \theta_2)^2} \\ &\quad + \frac{6\theta_1 \theta_2^2 \Gamma(\theta_1 - \theta_2)^3}{\Gamma(\theta_1 + 1)^3 \Gamma(3\theta_1 + 1) \Gamma(1 - \theta_2)^3}, \end{aligned}$$

and so on. The expression for $\langle Y_{\theta_1, \theta_2} \rangle$ given above is in accordance with (4.9). Higher moments have expressions of increasing complexity, involving gamma functions of more and more different arguments.

In the regime where θ_1 and θ_2 simultaneously go to 0, the moments of Y_{θ_1, θ_2} maintain a non-trivial rational dependence on the ratio $\alpha = \theta_2/\theta_1$, such that $0 < \alpha < 1$. The preceding expressions indeed reduce to

$$\begin{aligned} \lim_{\theta_1, \theta_2 \rightarrow 0} \langle Y_{\theta_1, \theta_2} \rangle &= \frac{1}{1 - \alpha}, \\ \lim_{\theta_1, \theta_2 \rightarrow 0} \langle Y_{\theta_1, \theta_2}^2 \rangle &= \frac{2(2 - 2\alpha + \alpha^2)}{(2 - \alpha)(1 - \alpha)^2}, \\ \lim_{\theta_1, \theta_2 \rightarrow 0} \langle Y_{\theta_1, \theta_2}^3 \rangle &= \frac{6(6 - 12\alpha + 12\alpha^2 - 5\alpha^3 + \alpha^4)}{(3 - \alpha)(2 - \alpha)(1 - \alpha)^3}. \end{aligned} \quad (5.20)$$

5.3 Behaviour at small values of Y_{θ_1, θ_2}

The behaviour of the density $f_{Y_{\theta_1, \theta_2}}(y)$ at small y can be extracted from (5.12) by noticing that $y \rightarrow 0$ corresponds to $\mu \rightarrow \infty$ and to $\lambda \rightarrow 0$ (see (5.13)).

Let us assume provisionally that the exponents θ_1 and θ_2 obey the inequality $\theta_1 + \theta_2 < 1$. The behaviour of $I(\lambda)$ at small λ can be obtained by inserting into (5.5) the behaviour of $\hat{f}_{X_{\theta_1}}(u)$ at large u , namely (see (2.31))

$$\hat{f}_{X_{\theta_1}}(u) \approx \frac{1}{\Gamma(1 - \theta_1)u}.$$

We thus obtain

$$I(\lambda) \approx \frac{\Gamma(1 - \theta_1 - \theta_2)}{\Gamma(1 - \theta_1)} \lambda^{\theta_1}.$$

The behaviour of $J(\lambda)$ and $K(\lambda)$ at small λ read (see (5.7), (5.8))

$$J(\lambda) \approx C\lambda^{-\theta_2}, \quad K(\lambda) \approx C\theta_2\lambda^{-\theta_2},$$

with

$$C = \frac{1}{\theta_1} \int_0^\infty du e^{-\lambda u^{1/\theta_1}} u^{-1-\theta_2/\theta_1} (1 - \hat{f}_{X_{\theta_1}}(u)).$$

An integration by parts followed by some algebra yields

$$C = \frac{\Gamma(1 - \theta_2/\theta_1)}{\theta_2} \langle X_{\theta_1}^{\theta_2/\theta_1} \rangle,$$

where X_{θ_1} has density $f_{X_{\theta_1}}(x)$ (see (2.29)). Extending the moment formula (2.33) to the non-integer value $k = \theta_2/\theta_1$, we obtain

$$C = \frac{\Gamma(1 - \theta_2/\theta_1)\Gamma(1 + \theta_2/\theta_1)}{\theta_2\Gamma(1 + \theta_2)},$$

and finally

$$\mathcal{R}(\lambda) \approx \frac{\Gamma(1 - \theta_1 - \theta_2)\Gamma(1 + \theta_2)}{\Gamma(1 - \theta_1)\Gamma(1 - \theta_2/\theta_1)\Gamma(1 + \theta_2/\theta_1)} \lambda^{\theta_1 + \theta_2}, \quad (5.21)$$

as long as the inequality $\theta_1 + \theta_2 < 1$ holds. When this inequality is not obeyed, the above singular term is still there, but it is subleading with respect to a regular term linear in λ .

The power-law singularity in (5.21) suggests to assume the power-law behaviour

$$f_{Y_{\theta_1, \theta_2}}(y) \approx Ay^\omega \quad (y \rightarrow 0). \quad (5.22)$$

Inserting this scaling expression into (5.13), performing the integrals, and identifying exponents and amplitudes with (5.21) yields

$$\omega = \frac{\theta_2}{\theta_1}$$

and

$$A = \frac{\Gamma(1 + \theta_2)}{\Gamma(1 - \theta_1)\Gamma(1 - \theta_2/\theta_1)\Gamma(1 + \theta_2/\theta_1)^2}.$$

The power-law behaviour (5.22) of the density of Y_{θ_1, θ_2} as $y \rightarrow 0$ is different from that of the density of X_θ , which goes to a finite constant as $x \rightarrow 0$ (see (2.31)). However, when $\theta_2 \rightarrow 0$, the exponent ω tends to zero, and the amplitude A matches with this constant.

5.4 Behaviour at large values of Y_{θ_1, θ_2}

In order to analyse the tail behaviour of the density $f_{Y_{\theta_1, \theta_2}}(y)$ for large values of y , we use the property that the latter behaviour is related to the asymptotic growth law of the moments $\langle Y_{\theta_1, \theta_2}^k \rangle$ at large k . The latter can be estimated by considering the denominator $\tilde{K}(\zeta)$ of the right-hand side $\tilde{\mathcal{R}}(\zeta)$ of (5.12), given by the power series (5.18). As ζ increases from 0 to 1, i.e., its radius of convergence, $\tilde{K}(\zeta)$ decreases from the positive value $\tilde{K}(0) = \Gamma(1 - \theta_2)$ to some finite negative value $\tilde{K}(1)$. There is therefore a critical value of ζ , denoted by ζ_c , such that

$$\tilde{K}(\zeta_c) = 0. \quad (5.23)$$

Both $\tilde{R}(\zeta)$ and $\tilde{L}(\zeta)$ therefore have a simple pole at ζ_c . As a consequence of (5.16), we have

$$\langle Y_{\theta_1, \theta_2}^k \rangle \sim \frac{k!}{\Gamma(k\theta_1 + 1)\zeta_c^k}, \quad (5.24)$$

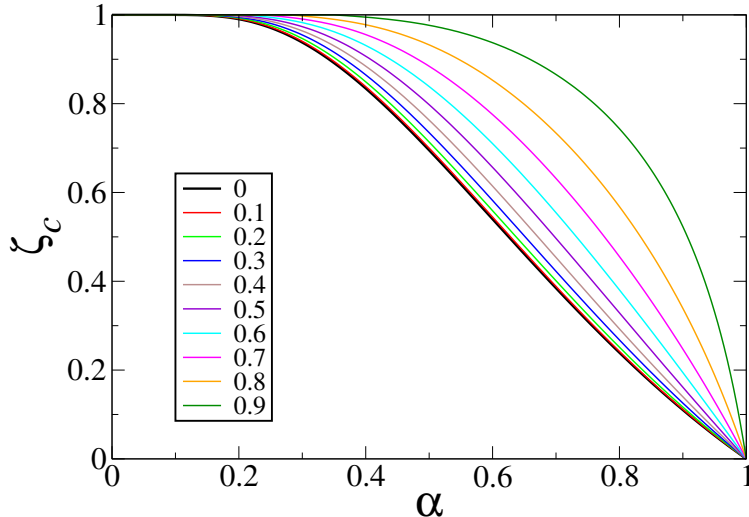


Fig. 4 Quantity ζ_c defined by (5.23) and entering the estimates (5.24) and (5.25), plotted against the ratio $\alpha = \theta_2/\theta_1$ for several values of θ_1 (see legend).

up to an inessential constant. Comparing the asymptotic estimate (5.24) to the exact expression (2.33) of the moments of X_θ , we are led to the conclusion that the tail behaviour of $f_{Y_{\theta_1, \theta_2}}(y)$ is obtained by replacing θ by θ_1 and x by the product $\zeta_c y$ in the compressed exponential estimate (2.32), obtaining thus

$$f_{Y_{\theta_1, \theta_2}}(y) \sim \exp\left(- (1 - \theta_1)(\theta_1^{\theta_1} \zeta_c y)^{1/(1-\theta_1)}\right). \quad (5.25)$$

This result depends on θ_2 only through the quantity ζ_c , defined in (5.23). The latter has a non-trivial dependence on θ_1 and θ_2 , decreasing from 1 to 0 as θ_2 is increased from 0 to θ_1 . It is plotted in figure 4 against the ratio $\alpha = \theta_2/\theta_1$ for several values of θ_1 (see legend). For $\theta_2 \rightarrow 0$, it can be argued that ζ_c departs from unity with an exponentially small singularity of the form

$$1 - \zeta_c \sim \exp\left(- \frac{|\ln(1 - \theta_1)|}{\theta_2}\right). \quad (5.26)$$

For $\theta_2 \rightarrow \theta_1$, the estimate (5.31), to be derived below, yields the linear behaviour

$$\zeta_c \approx \frac{\pi}{\sin \pi \theta_1} (\theta_1 - \theta_2). \quad (5.27)$$

In the regime where θ_1 and θ_2 simultaneously go to 0, the series (5.18) reduces to

$$\tilde{K}(\zeta) = -\alpha \sum_{k \geq 0} \frac{\zeta^k}{k - \alpha},$$

with $\alpha = \theta_2/\theta_1$, so that ζ_c keeps a non-trivial dependence on the ratio α (thick black curve in figure 4). The estimates (5.26) and (5.27) can be made more precise in this regime:

$$\begin{aligned} 1 - \zeta_c &= \exp\left(-\frac{1}{\alpha} + \frac{\pi^2 \alpha}{6} + \dots\right) & (\alpha \rightarrow 0), \\ \zeta_c &= (1 - \alpha) + (1 - \alpha)^2 + \dots & (\alpha \rightarrow 1). \end{aligned}$$

5.5 Three limiting situations

The three limiting situations of interest correspond to the edges of the triangular region D (see figure 2), that is, $\theta_2 \rightarrow 0$, $\theta_1 \rightarrow 1$, and $\theta_2 \rightarrow \theta_1$.

Limit $\theta_2 \rightarrow 0$

In this limit, the series (5.17) and (5.18) reduce to

$$\tilde{I}(\zeta) = \frac{1}{1-\zeta}, \quad \tilde{K}(\zeta) = 1, \quad \tilde{\mathcal{R}}(\zeta) = \frac{1}{1-\zeta}, \quad (5.28)$$

thus (5.16) yields

$$\langle Y_{\theta_1,0}^k \rangle = \frac{k!}{\Gamma(k\theta_1 + 1)}.$$

A comparison with (2.33) leads to the conclusion that, in this limit, the distribution of Y_{θ_1,θ_2} becomes that of X_{θ_1} (see (2.29)). In other words,

$$\lim_{\theta_2 \rightarrow 0} f_{Y_{\theta_1,\theta_2}}(y) = f_{X_{\theta_1}}(y). \quad (5.29)$$

This result can be understood as follows. When $\theta_2 \rightarrow 0$, the distribution of the time intervals $\mathbf{T}_1, \mathbf{T}_2, \dots$ becomes very broad, entailing that the largest of them, $\mathbf{T}_{\max} = \max(\mathbf{T}_1, \mathbf{T}_2, \dots)$, nearly spans the whole time interval $(0, t)$. More precisely, using the expression given in [35, eq. (3.34)] for the limiting ratio

$$\lim_{t \rightarrow \infty} \frac{1}{t} \langle \mathbf{T}_{\max} \rangle = \int_0^\infty \frac{dx}{1 + x^\theta e^x \int_0^x du u^{-\theta} e^{-u}},$$

it can be checked that this ratio goes to unity as $\theta \rightarrow 0$ (where θ stands for θ_2 in the present context), meaning that the entire process simplifies to the internal process over a time interval $\mathbf{T}_{\max} \approx t$. See also the comment below (4.9) on this limit.

Limit $\theta_1 \rightarrow 1$

In this limit, by inserting $\hat{f}_1(u) = e^{-u}$ (see (2.36)) into the integrals (5.5) and (5.8), and performing the latter integrals, we obtain, after some algebra,

$$\mathcal{R}(\lambda) = \frac{\lambda}{\lambda + 1}, \quad \tilde{\mathcal{R}}(\zeta) = \frac{1}{1-\zeta},$$

whereby (5.16) yields

$$\langle Y_{1,\theta_2}^k \rangle = 1.$$

In the limit $\theta_1 \rightarrow 1$, the distribution of Y_{θ_1,θ_2} thus becomes degenerate:

$$\lim_{\theta_1 \rightarrow 1} f_{Y_{\theta_1,\theta_2}}(y) = \delta(y - 1), \quad (5.30)$$

regardless of the value of θ_2 . The scaling variable X_θ has the same degenerate distribution as $\theta \rightarrow 1$ (see (2.36)).

Limit $\theta_2 \rightarrow \theta_1$

In this limit, the series (5.18) become singular, in the sense that the term corresponding to $k = 1$ diverges. Setting

$$\theta_2 = \theta_1 - \varepsilon,$$

we obtain

$$\begin{aligned} \tilde{I}(\zeta) &\approx \Gamma(1 - \theta_1), \\ \tilde{K}(\zeta) &\approx \Gamma(1 - \theta_1) - \frac{\zeta}{\Gamma(\theta_1)\varepsilon}, \\ \tilde{R}(\zeta) &\approx \frac{1}{1 - \frac{\sin \pi \theta_1}{\pi \varepsilon} \zeta}, \end{aligned} \quad (5.31)$$

whereby (5.16) yields

$$\langle Y_{\theta_1, \theta_1 - \varepsilon}^k \rangle \approx \left(\frac{\sin \pi \theta_1}{\pi \varepsilon} \right)^k \frac{k!}{\Gamma(k\theta_1 + 1)}.$$

A comparison with (2.33) leads to the following equivalence

$$Y_{\theta_1, \theta_1 - \varepsilon} \approx \frac{\sin \pi \theta_1}{\pi \varepsilon} X_{\theta_1}, \quad (5.32)$$

to leading order as $\varepsilon = \theta_1 - \theta_2 \rightarrow 0$, where X_{θ_1} is distributed according to (2.29), with exponent θ_1 . In other words,

$$f_{Y_{\theta_1, \theta_1 - \varepsilon}}(y) \approx \frac{\pi \varepsilon}{\sin \pi \theta_1} f_{X_{\theta_1}}\left(\frac{\pi \varepsilon}{\sin \pi \theta_1} y\right).$$

5.6 A measure of fluctuations

In order to obtain a quantitative measure of the size of the fluctuations of Y_{θ_1, θ_2} , we consider its reduced variance, denoted by

$$V = \frac{\text{Var } Y_{\theta_1, \theta_2}}{\langle Y_{\theta_1, \theta_2} \rangle^2} = \frac{\langle Y_{\theta_1, \theta_2}^2 \rangle}{\langle Y_{\theta_1, \theta_2} \rangle^2} - 1. \quad (5.33)$$

The explicit expressions (5.24) of the first two moments of Y yield

$$V = \frac{4\Gamma(\theta_1 + 1)^4 \Gamma(1 - \theta_2) \Gamma(2\theta_1 - \theta_2)}{\theta_1 \Gamma(2\theta_1 + 1)^2 \Gamma(\theta_1 - \theta_2)^2} + \frac{2\theta_2 \Gamma(\theta_1 + 1)^2}{\theta_1 \Gamma(2\theta_1 + 1)} - 1. \quad (5.34)$$

For a fixed θ_1 , V takes its maximal value,

$$V_{\max} = \frac{2\Gamma(\theta_1 + 1)^2}{\Gamma(2\theta_1 + 1)} - 1 = \frac{\langle X_{\theta_1}^2 \rangle}{\langle X_{\theta_1} \rangle^2} - 1 \quad (5.35)$$

at both endpoints of region D, namely for $\theta_2 \rightarrow 0$ and $\theta_2 \rightarrow \theta_1$, where Y_{θ_1, θ_2} becomes proportional to X_{θ_1} .

For intermediate values of θ_2 , the distribution of Y_{θ_1, θ_2} has less pronounced fluctuations, testified by a smaller value of the reduced variance V . Figure 5 shows plots of the ratio

$$W = \frac{V}{V_{\max}}$$

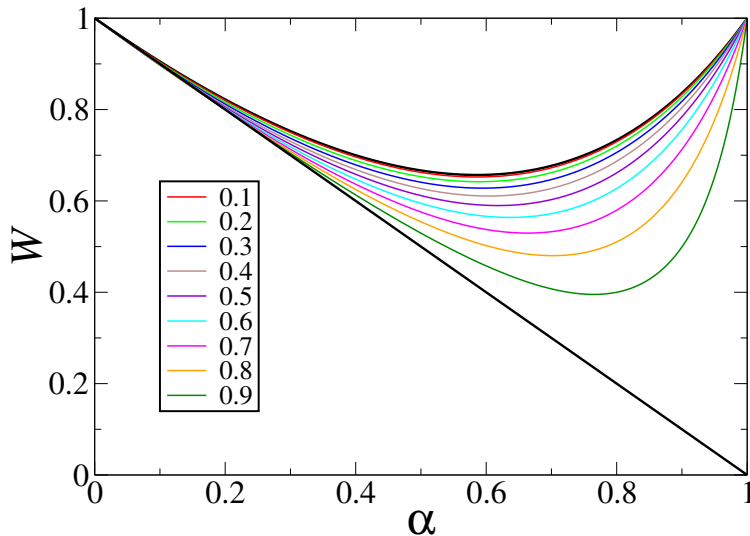


Fig. 5 Ratio $W = V/V_{\max}$, where V is the reduced variance of the scaling variable Y_{θ_1, θ_2} (see (5.33)), and V_{\max} is given by (5.35), plotted against the ratio $\alpha = \theta_2/\theta_1$ for several values of θ_1 (see legend). Thick black curves: limit expressions (5.36) and (5.37).

against the ratio $\alpha = \theta_2/\theta_1$ for several values of θ_1 (see legend). This quantity starts decreasing from its initial value $W = 1$ for $\alpha = 0$, goes through a minimum, and increases back to $W = 1$ for $\alpha = 1$. The minimum gets deeper and deeper as θ_1 is increased from 0 to 1. In the regime where θ_1 and θ_2 simultaneously go to 0, the expression (5.34) reduces to

$$W = \frac{2 - 3\alpha + 2\alpha^2}{2 - \alpha} = 1 - \frac{2\alpha(1 - \alpha)}{2 - \alpha}, \quad (5.36)$$

in accord with (5.20). This expression reaches a non-trivial minimum $W_{\min} = 4\sqrt{2} - 5 = 0.656854\dots$ for $\alpha = 2 - \sqrt{2} = 0.585786\dots$. In the opposite limit ($\theta_1 \rightarrow 1$), we have

$$W = 1 - \alpha, \quad (5.37)$$

testifying that the limits $\theta_1 \rightarrow 1$ and $\theta_2 \rightarrow \theta_1$ do not commute.

5.7 Integral representation of the density

The fundamental equation (5.12) also yields an integral representation of the density $f_{Y_{\theta_1, \theta_2}}(y)$. Its left-hand side has the structure of two nested Laplace transforms. Successively inverting these two transforms yields formally

$$f_{Y_{\theta_1, \theta_2}}(y) = \theta_1 \int \frac{d\lambda}{2\pi i \lambda} \int \frac{d\mu}{2\pi i} \mu^{\theta_1 - 1} e^{\lambda\mu + \mu^{\theta_1} y} \mathcal{R}(\lambda).$$

Changing integration variables from μ to $z = \lambda\mu$ and from λ to ζ (see (5.15)), we obtain

$$f_{Y_{\theta_1, \theta_2}}(y) = \int \frac{d\zeta}{2\pi i} \underbrace{\int \frac{dz}{2\pi i} z^{\theta_1 - 1} e^{z - z^{\theta_1} \zeta y}}_{\tilde{\mathcal{R}}(\zeta)} \tilde{\mathcal{R}}(\zeta).$$

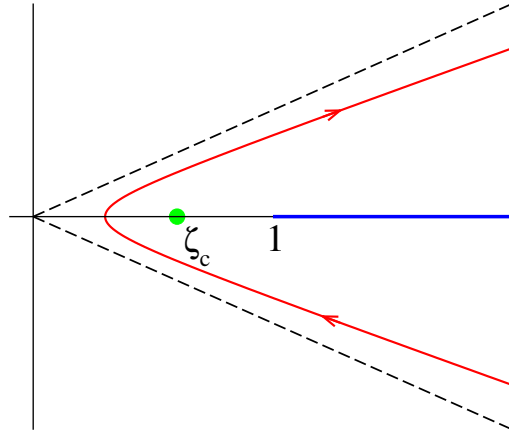


Fig. 6 The complex ζ -plane. Green symbol: pole of $\tilde{\mathcal{R}}(\zeta)$ at $\zeta = \zeta_c$. Blue line: branch cut of $\tilde{\mathcal{R}}(\zeta)$ from 1 to ∞ . Black dashed lines are at angles $\pm(1 - \theta_1)\pi/2$ beyond which the density $f_{X_{\theta_1}}(\zeta y)$ loses its exponential decay. Red curve: Integration contour Γ to be used in the representation (5.38).

The expression underlined with a brace is merely the integral representation (2.29) of the density $f_{X_{\theta_1}}(x)$, up to the replacement of the variable x by the product ζy . We have thus established the integral formula

$$f_{Y_{\theta_1, \theta_2}}(y) = \int_{\Gamma} \frac{d\zeta}{2\pi i} f_{X_{\theta_1}}(\zeta y) \tilde{\mathcal{R}}(\zeta), \quad (5.38)$$

which represents the density $f_{Y_{\theta_1, \theta_2}}(y)$ as a continuous superposition of densities of the type $f_{X_{\theta_1}}(x)$, with weight $\tilde{\mathcal{R}}(\zeta)$ given in (5.19). The integration contour Γ is described below and shown in figure 6.

Let us start by considering the limit of (5.38) as $\theta_2 \rightarrow 0$. The expression (5.28) shows that $\tilde{\mathcal{R}}(\zeta)$ has a simple pole at $\zeta = 1$, with residue -1 . In order to recover (5.29), the integration contour Γ must encircle this pole once in the clockwise direction.

In the generic situation ($0 < \theta_2 < \theta_1 < 1$), $\tilde{\mathcal{R}}(\zeta)$ has two singularities on the positive real axis, specifically a simple pole at $\zeta = \zeta_c$ between 0 and 1 and a branch cut extending from 1 to ∞ , as shown in figure 6. The density $f_{X_{\theta_1}}(\zeta y)$ has the compressed exponential decay (2.32) as long as the real part of $(\zeta y)^{1/(1-\theta_1)}$ is positive, i.e., ζ stays between the lines at angles $\pm(1 - \theta_1)\pi/2$. The integration contour Γ entering (5.38) should thus be placed as shown in the figure.

The integral representation (5.38) is very appealing conceptually. It is however not easy to handle in practice. The specific techniques introduced earlier are indeed far more efficient when exploring diverse facets of the distribution of Y_{θ_1, θ_2} , such as the calculation of moments, the behaviour of the density $f_{Y_{\theta_1, \theta_2}}(y)$ at small values of y , and the three limiting situations associated with the edges of region D.

The representation (5.38) simplifies in the special case where $\theta_1 = 1/2$. First of all, the density $f_{X_{1/2}}(x)$ has the simple form (2.35). The power series $\tilde{I}(\zeta)$ and $\tilde{K}(\zeta)$ (see (5.17), (5.18)) also become simpler. The arguments of all gamma functions are of the form $k/2 + c$ for various c . This suggests to consider separately even ($k = 2n$) and odd ($k = 2n + 1$) values of k .

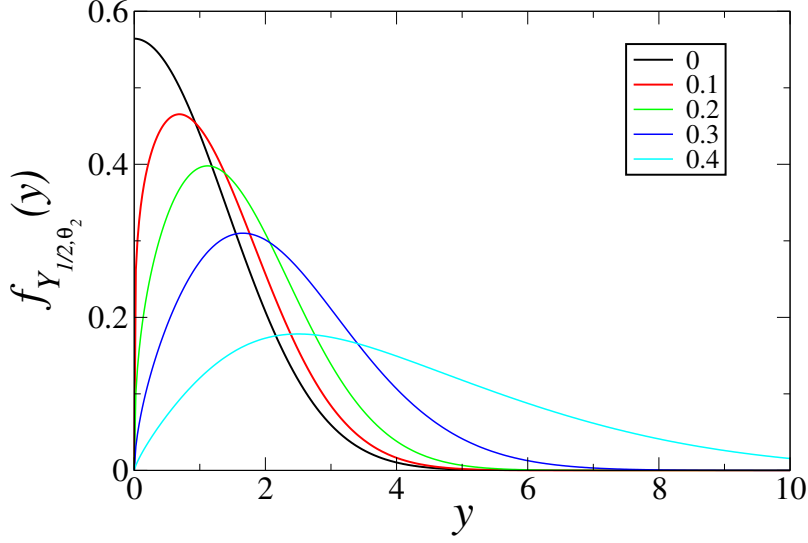


Fig. 7 Probability density $f_{Y_{1/2, \theta_2}}(y)$, obtained by means of the integral representation (5.38), using (2.35) and (5.40), for $\theta_1 = 1/2$ and several values of θ_2 (see legend).

We thus obtain

$$\begin{aligned} \tilde{I}_{\text{even}}(\zeta) &= \sum_{n \geq 0} \frac{\Gamma(n+1-\theta_2)}{n!} \zeta^{2n} = \Gamma(1-\theta_2)(1-\zeta^2)^{\theta_2-1}, \\ \tilde{I}_{\text{odd}}(\zeta) &= \sum_{n \geq 0} \frac{\Gamma(n+\frac{3}{2}-\theta_2)}{\Gamma(n+\frac{3}{2})} \zeta^{2n+1} = \frac{\Gamma(\frac{3}{2}-\theta_2)}{\Gamma(\frac{3}{2})} \zeta F\left(\frac{3}{2}-\theta_2, 1; \frac{3}{2}; \zeta^2\right), \\ \tilde{K}_{\text{even}}(\zeta) &= -\theta_2 \sum_{n \geq 0} \frac{\Gamma(n-\theta_2)}{n!} \zeta^{2n} = \Gamma(1-\theta_2)(1-\zeta^2)^{\theta_2}, \\ \tilde{K}_{\text{odd}}(\zeta) &= -\theta_2 \sum_{n \geq 0} \frac{\Gamma(n+\frac{1}{2}-\theta_2)}{\Gamma(n+\frac{3}{2})} \zeta^{2n+1} = -\frac{\theta_2 \Gamma(\frac{1}{2}-\theta_2)}{\Gamma(\frac{3}{2})} \zeta F\left(\frac{1}{2}-\theta_2, 1; \frac{3}{2}; \zeta^2\right), \end{aligned} \quad (5.39)$$

where $F(a, b; c; z)$ is the hypergeometric series. Thus (5.19) reads

$$\tilde{\mathcal{R}}(\zeta) = \frac{\tilde{I}_{\text{even}}(\zeta) + \tilde{I}_{\text{odd}}(\zeta)}{\tilde{K}_{\text{even}}(\zeta) + \tilde{K}_{\text{odd}}(\zeta)}. \quad (5.40)$$

The formulas (2.35), (5.39) and (5.40) turn the representation (5.38) into an efficient tool to evaluate the density $f_{Y_{1/2, \theta_2}}(y)$ numerically. Figure 7 shows the distribution thus obtained, for several values of θ_2 (see legend). The general trend is that, as θ_2 is increased from 0 to θ_1 , the density $f_{Y_{\theta_1, \theta_2}}(y)$ broadens while its maximum shifts to the right.

To close, we mention that the representation (5.38) simplifies whenever $\theta_1 = p/q$ is a rational number. First, the density $f_{X_\theta}(x)$ is related to the stable Lévy law of index θ (see (2.30)), which is known to admit explicit expressions in terms of special functions whenever θ is rational [36, 37]. Furthermore, the series $\tilde{I}(\zeta)$ and $\tilde{K}(\zeta)$ can be expressed as linear combinations of q hypergeometric series, by generalising the above construction. The resulting expressions however soon become pretty cumbersome.

6 Two special cases

6.1 Poissonian internal process

When $\rho(\tau)$ is exponential, of the form

$$\rho(\tau) = \lambda e^{-\lambda\tau}, \quad \hat{\rho}(s) = \frac{\lambda}{\lambda + s}, \quad (6.1)$$

the internal renewal process is a Poisson process, implying, as shown below, that the statistics of \mathcal{N}_t is Poisson, too, regardless of the distribution $f(T)$ characterising the external process. In the phase diagram of figure 2, this case lies on the right boundaries of regions A and B, where $\theta_1 = \infty$.

For the internal process, the expression (2.15) simplifies to

$$\hat{Z}(z, s) = \frac{1}{s + (1 - z)\lambda}, \quad (6.2)$$

hence

$$Z(z, t) = e^{(z-1)\lambda t}, \quad (6.3)$$

implying that the number N_t of renewals up to time t has a Poisson distribution with parameter λt ,

$$\mathbb{P}(N_t = n) = e^{-\lambda t} \frac{(\lambda t)^n}{n!}. \quad (6.4)$$

For the entire process, we have

$$\begin{aligned} \hat{\varphi}(z, s) &= \int_0^\infty dT f(T) e^{-sT} e^{(z-1)\lambda T} = \hat{f}(s + (1 - z)\lambda), \\ \hat{\psi}(z, s) &= \int_0^\infty dT \Phi(T) e^{-sT} e^{(z-1)\lambda T} = \hat{\Phi}(s + (1 - z)\lambda) = \frac{1 - \hat{f}(s + \lambda(1 - z))}{s + \lambda(1 - z)}, \end{aligned}$$

and (3.9) simplifies to

$$\hat{\mathcal{Z}}(z, s) = \frac{1}{s + (1 - z)\lambda},$$

which is identical to (6.2), implying that \mathcal{N}_t has a Poisson distribution (6.4) with parameter λt , regardless of the external density $f(T)$. This result has the following interpretation. As a consequence of (6.3), the numbers of points in the successive intervals $\mathbf{T}_1, \mathbf{T}_2, \dots, \mathbf{B}_t$ have independent Poisson distributions, with respective parameters $\lambda\mathbf{T}_1, \lambda\mathbf{T}_2, \dots, \lambda\mathbf{B}_t$, implying that their sum \mathcal{N}_t has a Poisson distribution whose parameter is the sum of all parameters, i.e., λt .

We have in particular, using the fact that $\lambda = 1/\langle\tau\rangle$,

$$\langle\mathcal{N}_t\rangle = \frac{t}{\langle\tau\rangle}.$$

In region A, this result is in agreement with (4.2), since $\langle N_{\mathbf{T}} \rangle = \langle \mathbf{T} \rangle / \langle \tau \rangle$, while for region B, this result is precisely (4.6).

6.2 Poissonian resetting and dressed renewal process

Poissonian resetting, which is the simplest—and the most studied—case of stochastic resetting, corresponds to the circumstance where $f(T)$ is exponential, of the form

$$f(T) = re^{-rT}, \quad (6.5)$$

hence $\Phi(T) = e^{-rT}$. In the phase diagram of figure 2, this case lies on the upper boundary of region A, where $\theta_2 = \infty$.

The general results of section 3 also simplify in this situation. We have indeed

$$\hat{\varphi}(z, s) = r\hat{Z}(z, r + s), \quad \hat{\psi}(z, s) = \hat{Z}(z, r + s),$$

implying that (3.9) takes on the familiar form

$$\hat{Z}(z, s) = \frac{\hat{Z}(z, r + s)}{1 - r\hat{Z}(z, r + s)}, \quad (6.6)$$

which could alternatively have been obtained from a renewal equation⁶ and where $\hat{Z}(z, s)$ is given by (2.15). Hence

$$\hat{Z}(z, s) = \frac{1 - \hat{\rho}(r + s)}{s + (r - (r + s)z)\hat{\rho}(r + s)}. \quad (6.7)$$

When $r \rightarrow 0$ the replication disappears and we consistently retrieve (2.15). By differentiating (6.7) with respect to z at $z = 1$, we obtain in particular

$$\mathcal{L}_t \langle \mathcal{N}_t \rangle = \frac{(r + s)\hat{\rho}(r + s)}{s^2(1 - \hat{\rho}(r + s))},$$

entailing that, in the long-time regime,

$$\langle \mathcal{N}_t \rangle \approx \frac{r\hat{\rho}(r)}{1 - \hat{\rho}(r)} t = \frac{\hat{\rho}(r)}{1 - \hat{\rho}(r)} \frac{t}{\langle \mathbf{T} \rangle}, \quad (6.8)$$

which is of the form (4.2) or (4.3).

Remarkably enough, the expression (6.7) is of the form (2.15), where $\hat{\rho}(s)$ is replaced by the expression

$$\hat{\rho}^{(r)}(s) = \frac{(r + s)\hat{\rho}(r + s)}{s + r\hat{\rho}(r + s)}. \quad (6.9)$$

We conclude that, in the present circumstance of Poissonian resetting, the events of the internal process (the crosses in figure 1) are exactly described by a single renewal process, defined by the dressed density $\rho^{(r)}(\tau)$, depending on the resetting rate r and on the distribution $\rho(\tau)$. This is the common probability density of the dressed interarrival times $\tau_1^{(r)}, \tau_2^{(r)}, \dots$, such that

$$\hat{\rho}^{(r)}(s) = \langle e^{-s\tau^{(r)}} \rangle.$$

As $r \rightarrow 0$, the dressed density $\rho^{(r)}(\tau)$ reduces to the bare one $\rho(\tau)$, as expected.

Notice that, if one substitutes (2.13) in (6.9), the Laplace transform of the dressed survival probability $\hat{R}^{(r)}(s) = (1 - \rho^{(r)}(s))/s$ takes on the familiar form (see, e.g., [9])

$$\hat{R}^{(r)}(s) = \frac{\hat{R}(r + s)}{1 - r\hat{R}(r + s)}.$$

Considerations on the survival probability and the first-passage time in the general case of an arbitrary resetting density $f(T)$ will be presented in section 7.

⁶ See [9] and references therein for similar relationships with other observables.

In the particular case where $\rho(\tau)$ is the exponential distribution (6.1), we recover $\rho^{(x)}(\tau) = \rho(\tau)$, irrespective of the rate r , in agreement with the results of section 6.1. The simplest non-trivial example is the case where $\rho(\tau)$ is the convolution of two exponentials, namely

$$\rho(\tau) = \lambda^2 \tau e^{-\lambda\tau}, \quad (6.10)$$

leading to

$$\rho^{(x)}(\tau) = \frac{\lambda^2}{\omega} e^{-(\lambda+r/2)\tau} \sinh \omega\tau, \quad \omega = \frac{\sqrt{r(4\lambda+r)}}{2}.$$

The dressed density $\rho^{(x)}(\tau)$ generically has an exponential decay,

$$\rho^{(x)}(\tau) \sim e^{-\mu\tau},$$

where the decay rate μ is the opposite of the nearest zero of the denominator of (6.9)⁷, obeying $\mu = r\hat{\rho}(r - \mu)$. All moments of $\rho^{(x)}(\tau)$ are therefore finite. We have in particular (see (6.8))

$$\langle \tau^{(x)} \rangle = \frac{1 - \hat{\rho}(r)}{r\hat{\rho}(r)}.$$

This expression is expected to be related to $\langle \tau \rangle$ at weak resetting. More precisely, when $\langle \tau \rangle$ is finite, that is to say if $\theta_1 > 1$, then $\langle \tau^{(x)} \rangle$ does indeed converge to $\langle \tau \rangle$ as $r \rightarrow 0$. Conversely, if $\langle \tau \rangle$ is infinite, meaning $\theta_1 < 1$, $\langle \tau^{(x)} \rangle$ diverges as $r \rightarrow 0$, according to

$$\langle \tau^{(x)} \rangle \approx \frac{\Gamma(1 - \theta_1) \tau_0^{\theta_1}}{r^{1-\theta_1}}. \quad (6.11)$$

This expression is to be compared to the marginal mean of a single time interval, given by (2.39), with $\theta = \theta_1 < 1$. The two expressions (2.39) and (6.11) are similar, with $1/r$ playing the role of the observation time. In particular, both prefactors diverge in the $\theta_1 \rightarrow 1$ limit.

7 First-passage time under restart

In the case of Poissonian resetting (see section 6.2), the intervals of time $\tau_1^{(x)}, \tau_2^{(x)}, \dots$ between successive internal events (shown as crosses in figure 1) are iid and drawn from the dressed density $\rho^{(x)}(\tau)$. This means that $\tau_2^{(x)}, \tau_3^{(x)}, \dots$ are probabilistic copies of the first interval, $\tau_1^{(x)}$, which itself is the time of the first occurrence of a renewal, or first-passage time for short, *in the presence of resetting*.

In the general case where the external process has an arbitrary density $f(T)$, there is no such renewal description for the sequence of crosses in terms of a dressed density. Nevertheless, the time of the first occurrence of a renewal for the process with resetting, or first-passage time, remains well defined, even if the subsequent time intervals between crosses are now no longer probabilistic copies of this first interval. Hereafter, we shall keep the same notations $\tau_1^{(x)}$ and $\rho^{(x)}(\tau)$ to refer to this first-passage time and its probability density. The latter density can be derived in two complementary ways, as we now show.

We start from the observation that

$$\mathcal{Z}(0, t) = \mathbb{P}(\mathcal{N}_t = 0) = \mathbb{P}(\tau^{(x)} > t) = \int_t^\infty d\tau \rho^{(x)}(\tau),$$

⁷ In the example (6.10), $\mu = \lambda + r/2 - \omega$ decreases continuously from λ to 0 as r is increased.

hence, in Laplace space,

$$\hat{\mathcal{Z}}(0, s) = \mathcal{L}_t \mathcal{Z}(0, t) = \mathcal{L}_t \mathbb{P}(\mathcal{N}_t = 0) = \frac{1 - \hat{\rho}^{(r)}(s)}{s}. \quad (7.1)$$

We now refer to (3.7), (3.8) and (3.9) to obtain

$$\hat{\mathcal{Z}}(0, s) = \frac{\hat{\psi}(0, s)}{1 - \hat{\varphi}(0, s)}, \quad (7.2)$$

with

$$\hat{\varphi}(0, s) = \int_0^\infty dT e^{-sT} f(T) Z(0, T) = \int_0^\infty dT e^{-sT} f(T) R(T) \quad (7.3)$$

and

$$\hat{\psi}(0, s) = \int_0^\infty dT e^{-sT} \Phi(T) R(T). \quad (7.4)$$

Put together, the above equations lead to the desired result

$$\hat{\rho}^{(r)}(s) = \langle e^{-s\tau_1^{(r)}} \rangle = \frac{\int_0^\infty dT e^{-sT} \rho(T) \Phi(T)}{1 - \int_0^\infty dT e^{-sT} f(T) R(T)}. \quad (7.5)$$

The identity

$$\int_0^\infty dT (\rho(T) \Phi(T) + f(T) R(T)) = 1,$$

which simply states that $\mathbb{P}(\tau < \mathbf{T}) + \mathbb{P}(\tau > \mathbf{T}) = 1$, allows one to check that $\hat{\rho}^{(r)}(0) = 1$, i.e., that the density $\rho^{(r)}(\tau)$ is normalised. In the particular case where $f(T)$ is exponential (see (6.5)), (7.5) becomes (6.9), as it should be.

By taking the derivative of (7.5) with respect to s at $s = 0$, the following formal expression for the mean value of $\tau_1^{(r)}$ is obtained:

$$\langle \tau_1^{(r)} \rangle = \frac{\int_0^\infty dT T R(T) \Phi(T)}{\int_0^\infty dT \rho(T) \Phi(T)}.$$

This expression is convergent, so that the mean first-passage time is well defined, when the tail exponents obey the inequality

$$\theta_1 + \theta_2 > 1.$$

Interestingly enough, the above inequality does not show up in the construction of the phase diagram of figure 2. This discrepancy lies in the fact that the nature of $\tau_1^{(r)}$ is that of a ‘boundary’ observable, whereas the phase diagram concerns the ‘bulk’ observable \mathcal{N}_t . The same observation applies for the statistics of the ‘boundary’ observable N_{B_t} (see section 8).

In order to better understand the meaning of the result (7.5), we present an alternative derivation, inspired by [38, 19, 13]. The first-passage time $\tau_1^{(r)}$ obeys the recursion

$$\tau_1^{(r)} = \begin{cases} \tau & \text{if } \tau < \mathbf{T}, \\ \mathbf{T} + (\tau_1^{(r)})' & \text{if } \tau > \mathbf{T}, \end{cases} \quad (7.6)$$

where $(\tau_1^{(r)})'$ is an independent copy of $\tau_1^{(r)}$. Let

$$p = \mathbb{P}(\tau < \mathbf{T}) = \int_0^\infty dT \rho(T) \Phi(T). \quad (7.7)$$

Iterating (7.6), we obtain

$$\tau_1^{(r)} = \tilde{\mathbf{T}}_1 + \cdots + \tilde{\mathbf{T}}_k + \tilde{\tau}_{k+1},$$

with probability $p(1-p)^k$, where the tilde indicates that these random variables are conditioned by the inequalities on the right-hand side of (7.6). We thus infer that

$$\hat{\rho}^{(x)}(s) = \sum_{k \geq 0} p(1-p)^k \hat{f}_{\tilde{T}}(s)^k f_{\tilde{\tau}}(s) = \frac{p f_{\tilde{\tau}}(s)}{1 - (1-p) \hat{f}_{\tilde{T}}(s)},$$

where

$$f_{\tilde{\tau}}(\tau) = \frac{\rho(\tau) \Phi(\tau)}{p}, \quad f_{\tilde{T}}(T) = \frac{f(T) R(T)}{1-p}.$$

which, again, lead to (7.5). We refer to [38, 19, 13] for further considerations on the topic of first passage under restart.

Yet another derivation of (7.5), based on a renewal equation for the survival probability $\mathbb{P}(\tau_1^{(x)} > t)$, can be found in [9] (see also references therein).

8 Number of internal renewals N_{B_t} in the last interval

As mentioned earlier, nested renewal processes have been initially introduced in the context of reliability problems [6, 39, 40, 41]. Studying the statistics of N_{B_t} was one of the primary aims of [6]. This quantity represents the number of internal renewals in the interval B_t , which is the backward recurrence time for the external renewal process (see figure 1). In [6], the study was restricted to the case of thin-tailed distributions for both the internal and external renewal processes, where the statistics of N_{B_t} becomes stationary at long times. Here we shall be interested in exploring the phase diagram in the whole θ_1 - θ_2 -plane.

8.1 On the statistics of N_{B_t}

The statistics of N_{B_t} can be determined by utilising (3.13), (3.14), (3.15) and (3.16).

Let us focus on the asymptotic behaviour of its mean $\langle N_{B_t} \rangle$. Figure 8 gives a summary of the results obtained using techniques similar to those outlined in section 4, as elaborated below.

Beforehand, to gain an intuitive understanding of this phase diagram, one can compare the mean values of the two time intervals: B_t for the resetting process, and τ_t for the internal renewal process. For the former, we have [24]

$$\langle B_t \rangle \sim \begin{cases} O(1) & \theta_2 > 2, \\ t^{2-\theta_2} & 1 < \theta_2 < 2, \\ t & \theta_2 < 1, \end{cases}$$

while (see (2.39))

$$\langle \tau_t \rangle \sim \begin{cases} O(1) & \theta_1 > 1, \\ t^{1-\theta_1} & \theta_1 < 1, \end{cases}$$

for the latter. For instance, when both exponents are greater than unity, $\langle N_{B_t} \rangle \sim \langle B_t \rangle / \langle \tau_t \rangle \sim O(1)$, when both exponents are less than unity, $\langle N_{B_t} \rangle \sim \langle B_t \rangle / \langle \tau_t \rangle \sim t^{\theta_1}$, and so on.

A more detailed approach is as follows. The number of renewals N_{B_t} in the random interval B_t can be expressed, asymptotically, as

$$N_{B_t} \approx \begin{cases} \frac{B_t}{\langle \tau \rangle}, & \theta_1 > 1, \\ \frac{X_{\theta_1}}{\Gamma(1-\theta_1)} \left(\frac{B_t}{\tau_0} \right)^{\theta_1} & \theta_1 < 1 \end{cases} \quad (8.1)$$

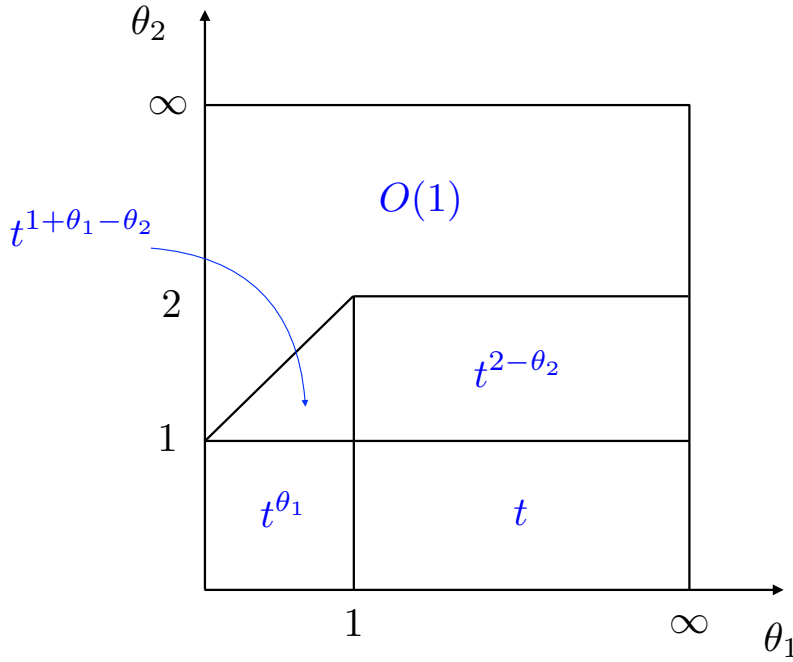


Fig. 8 Asymptotic behaviour of the mean number of internal renewals $\langle N_{B_t} \rangle$ in the interval B_t , the backward recurrence time of the external process.

where, asymptotically,

$$B_t \approx \begin{cases} B_{\text{eq}} & \theta_2 > 1, \\ t^\beta & \theta_2 < 1. \end{cases} \quad (8.2)$$

The densities of the expressions in the right-hand side of this equation are

$$f_{B,\text{eq}}(B) = \frac{\Phi(B)}{\langle \mathbf{T} \rangle} \approx \frac{1}{\langle \mathbf{T} \rangle} \left(\frac{T_0}{B} \right)^{\theta_2},$$

for the first line, while the density of the rescaled random variable β is

$$f_\beta(x) = \frac{\sin \pi \theta}{\pi} x^{-\theta} (1-x)^{\theta-1} = \beta_{1-\theta, \theta}(x) \quad (0 < x < 1),$$

where

$$\beta_{a,b}(x) = \frac{\Gamma(a+b)}{\Gamma(a)\Gamma(b)} x^{a-1} (1-x)^{b-1}$$

is the beta distribution on $[0, 1]$ [24].

The asymptotic expressions of $\langle N_{B_t} \rangle$ follow readily from (8.1) and (8.2), using (3.16) or, equivalently, in direct space,

$$\langle N_{B_t} \rangle = \int_0^t dB f_{B_t}(t, B) \langle N_B \rangle,$$

where, in $\langle N_B \rangle$, the temporal interval B is fixed.

Thus, if $\theta_1 > 1$,

$$\langle N_{B_t} \rangle \approx \begin{cases} \frac{\langle \mathbf{T}^2 \rangle}{2\langle \boldsymbol{\tau} \rangle \langle \mathbf{T} \rangle}, & \theta_2 > 2, \\ \frac{T_0^\theta}{(2 - \theta_2)\langle \boldsymbol{\tau} \rangle \langle \mathbf{T} \rangle} t^{2-\theta_2}, & 1 < \theta_2 < 2, \\ \frac{1 - \theta_2}{\langle \boldsymbol{\tau} \rangle} t, & \theta_2 < 1. \end{cases}$$

If $\theta_1 < 1$, we have

$$\langle N_{B_t} \rangle \approx \begin{cases} \frac{I_2(0)}{\langle \mathbf{T} \rangle}, & 1 + \theta_1 < \theta_2, \\ \frac{\sin \pi \theta_1 T_0^{\theta_2}}{\pi \theta_1 \tau_0^{\theta_1} \langle \mathbf{T} \rangle} \frac{t^{1+\theta_1-\theta_2}}{1 + \theta_1 - \theta_2}, & 1 < \theta_2 < 1 + \theta_1, \\ \frac{\sin \pi \theta_1}{\pi \theta_1} \langle \beta^{\theta_1} \rangle \left(\frac{t}{\tau_0} \right)^{\theta_1}, & \theta_2 < 1. \end{cases}$$

The constant numerator appearing in the first line is the finite limit of $I_2(s)$ when $s \rightarrow 0$,

$$I_2(0) = \int_0^\infty dT \Phi(T) \langle N_T \rangle.$$

Finally, notice that N_{B_t} contributes to the total sum \mathcal{N}_t , given in (3.3), in regions B and D only. However, in both regions, its behaviour differs from that of \mathcal{N}_t . In region B, \mathcal{N}_t has negligible fluctuations around its mean, while $N_{B_t} \sim t\beta$ keeps fluctuating, which means that the fluctuations of the sum of the M_t first terms in (3.3) compensate those of N_{B_t} . In region D, $\mathcal{N}_t \sim Y_{\theta_1, \theta_2} t^{\theta_1}$, while $N_{B_t} \sim X_{\theta_1} \beta^{\theta_1} t^{\theta_1}$, meaning that all the complexity of the behaviour of \mathcal{N}_t lies in the sum of the M_t first terms in (3.3).

8.2 Continuous time random walk subject to resetting

As mentioned earlier (see section 2), a continuous time random walk subject to resetting involves two nested renewal processes. The process considered in [6], and recalled in section 1, is equivalent to a continuous time random walk, where the shocks, causing damages of magnitude η_1, η_2, \dots , with common density f_η , correspond to the jumps. The cumulative damage of the component in use is to be identified with the position of the walker at time t , that is,

$$X_t = \eta_1 + \eta_2 + \dots + \eta_{N_{B_t}},$$

with probability density

$$f_{X_t}(x) = \sum_{n \geq 0} (f_{\eta^\star})^n(x) \mathbb{P}(N_{B_t} = n).$$

Assuming, for instance, that the distribution of the steps η_1, η_2, \dots is symmetric, one easily finds that the mean squared displacement of the walker reads

$$\langle X_t^2 \rangle = \langle N_{B_t} \rangle \langle \eta^2 \rangle.$$

The computation of the mean squared displacement for a continuous time random walk under power-law resetting has previously been addressed in [20], resulting in a phase diagram for the asymptotic time dependence of this quantity in the θ_1 - θ_2 -plane. This phase diagram corresponds precisely to the one depicted in figure 8.

Acknowledgements It is a pleasure to thank Pierre Vanhove for an interesting discussion.

References

1. Feller, W.: An Introduction to Probability Theory and its Applications, vol. 1. Wiley, New York (1968)
2. Feller, W.: An Introduction to Probability Theory and its Applications, vol. 2. Wiley, New York (1971)
3. Cox, D.R.: Renewal Theory. Methuen, London (1962)
4. Cox, D.R., Miller, H.D.: The Theory of Stochastic Processes, vol. 134. CRC Press, Boca Raton (1977)
5. Grimmett, G., Stirzaker, D.: Probability and random processes. Oxford University Press, Oxford (2020)
6. Ansell, J., Bendell, A., Humble, S.: Nested renewal processes. *Adv. Appl. Prob.* **12**, 880–892 (1980)
7. Paschalis, A., Molnar, P., Fatichi, S., Burlando, P.: On temporal stochastic modeling of precipitation, nesting models across scales. *Adv. Water Res.* **63**, 152–166 (2014)
8. Montero, M., Masó-Puigdellosas, A., Villarroel, J.: Continuous-time random walks with reset events: historical background and new perspectives. *Eur. Phys. J. B* **90**, 176 (2017)
9. Evans, M.R., Majumdar, S.N., Schehr, G.: Stochastic resetting and applications. *J. Phys. A: Math. Theor.* **53**, 193001 (2020)
10. Gupta, S., Jayannavar, A.M.: Stochastic resetting: A (very) brief review. *Front. Phys.* **10**, 789097 (2022)
11. Pólya, G.: Über eine Aufgabe der Wahrscheinlichkeitsrechnung betreffend die Irrfahrt im Straßennetz. *Math. Annalen* **84**, 149–160 (1921)
12. Majumdar, S.N., Sabhapandit, S., Schehr, G.: Random walk with random resetting to the maximum position. *Phys. Rev. E* **92**(5), 052126 (2015)
13. Bonomo, O.L., Pal, A.: First passage under restart for discrete space and time: application to one-dimensional confined lattice random walks. *Phys. Rev. E* **103**(5), 052129 (2021)
14. Godrèche, C., Luck, J.M.: Maximum and records of random walks with stochastic resetting. *J. Stat. Mech.* **2022**(6), 063202 (2022)
15. Kumar, A., Pal, A.: Universal framework for record ages under restart. *Phys. Rev. Lett.* **130**(15), 157101 (2023)
16. Godrèche, C., Luck, J.M.: Returns to the origin of the Pólya walk with stochastic resetting (2023). Preprint arXiv:2300.00000
17. Nagar, A., Gupta, S.: Diffusion with stochastic resetting at power-law times. *Phys. Rev. E* **93**(6), 060102 (2016)
18. Eule, S., Metzger, J.: Non-equilibrium steady states of stochastic processes with intermittent resetting. *New J. Phys.* **18**(3), 033006 (2016)
19. Pal, A., Reuveni, S.: First passage under restart. *Phys. Rev. Lett.* **118**(3), 030603 (2017)
20. Bodrova, A.S., Sokolov, I.M.: Continuous-time random walks under power-law resetting. *Phys. Rev. E* **101**(6), 062117 (2020)
21. Shkilev, V.P., Sokolov, I.M.: Subdiffusive continuous time random walks with power-law resetting. *J. Phys. A: Math. Theor.* **55**(48), 484003 (2022)
22. Mishra, S., Basu, U.: Symmetric exclusion process under stochastic power-law resetting. *J. Stat. Mech.* **2023**(5), 053202 (2023)
23. Barkai, E., Flaquer-Galmes, R., Méndez, V.: Ergodic properties of Brownian motion under stochastic resetting (2023). Preprint arXiv:2306.13621
24. Godrèche, C., Luck, J.M.: Statistics of the occupation time of renewal processes. *J. Stat. Phys.* **104**, 489–524 (2001)
25. Montroll, E.W., Weiss, G.H.: Random walks on lattices, II. *J. Math. Phys.* **6**, 167–181 (1965)
26. Weiss, G.H.: Aspects and Applications of Random Walks. North-Holland, Amsterdam (1994)
27. Landau, L.D.: On the energy loss of fast particles by ionization. *J. Phys.* **8**, 201–205 (1944)
28. Pollard, H.: The completely monotonic character of the Mittag-Leffler function $E_\alpha(-x)$. *Bull. Amer. Math. Soc.* **54**, 1115–1116 (1948)
29. Godrèche, C., Luck, J.M.: On sequences of records generated by planar random walks. *J. Phys. A: Math. Theor.* **54**, 325003 (2021)
30. Haubold, H.J., Mathai, A.M., Saxena, R.K.: Mittag-Leffler functions and their applications. *J. Appl. Math.* **2011**, 298628 (2011)
31. Darling, D.A., Kac, M.: On occupation times for Markoff processes. *Trans. Amer. Math. Soc.* **84**(2), 444–458 (1957)
32. Pillai, R.N.: On Mittag-Leffler functions and related distributions. *Ann. Inst. Statist. Math.* **42**, 157–161 (1990)
33. Cox, D.R.: On the number of renewals in a random interval. *Biometrika* **47**, 449–452 (1960)
34. Kilbas, A.A., Saigo, M., Trujillo, J.J.: On the generalized Wright function. *Fract. Calc. Appl. Anal.* **5**, 437–460 (2002)
35. Godrèche, C., Majumdar, S.N., Schehr, G.: Statistics of the longest interval in renewal processes. *J. Stat. Mech.* **2015**(3), P03014 (2015)
36. Penson, K.A., Górska, K.: Exact and explicit probability densities for one-sided Lévy stable distributions. *Phys. Rev. Lett.* **105**, 210604 (2010)
37. Górska, K., Penson, K.A.: Lévy stable distributions via associated integral transform. *J. Math. Phys.* **53**, 053302 (2012)
38. Reuveni, S.: Optimal stochastic restart renders fluctuations in first passage times universal. *Phys. Rev. Lett.* **116**(17), 170601 (2016)

-
39. Bendell, A., Scott, N.H.: Nested renewal processes with special Erlangian densities. *Oper. Res.* **32**(6), 1345–1357 (1984)
 40. Bendell, A., Humble, S.: A reliability model with states of partial operation. *Nav. Res. Logist. Q.* **32**(3), 509–535 (1985)
 41. Degbotse, A.T., Nachlas, J.A.: Use of nested renewals to model availability under opportunistic maintenance policies. In: *Annual Reliability and Maintainability Symposium, 2003 Proceedings*, pp. 344–350 (2003)